IMPROVED SEMI-CONDUCTOR LASER DEVICE, OPERATING, AT ROOM TEMPERATURE, WITH AN ARRAY OF THREE LASERS IN THE SPATIALLY COHERENT, FREE RUNNING MODE

Final Report
Contract No. NAS 8-30543

July 30, 1975

Prepared By

E.M. Rutz
for
National Aeronautics and Space Administration
Huntsville, Alabama

Federal Systems Division
INTERNATIONAL BUSINESS MACHINES CORPORATION
Gaithersburg, Maryland 20760

CONTENTS

1. Introduction

In accordance with IBM's proposal on an "Improved diffraction Limited Semiconductor Laser Device, for Room Temperature Operation, With Increased Average Pulse Power", of August 14, 1973, IBM has increased the peak pulse power by operating an array of three homostructure Ga As lasers in the laser device. A spatial filter in the laser device selects the spatially coherent, free running, mode. The optical peak power is 5 watts, that is three times the peak power of a single laser in the array. The far-field distribution of the three laser array is a single Gaussian beam of spatial coherence without sidelobes or grating lobes. The length of the optical pulses of spatial coherence was increased to 200 ns by improved heat transfer from the p-n junctions of the lasers to the metal housing of the pulse transformer and by doubling the core area and increasing the turns of the primary windings of the pulse transformer. The mechanical stability of the laser device was improved and the transition from mechanical alignment to electro-mechanical alignment control, was facilitated.

2. SUMMARY

The objective of the contract NAS 8-30543 is to increase the average pulse power, at room temperature, of the diffraction limited semi-conductor laser device, developed by IBM under contract NAS 8-11974, through the use of arrays of improved semi-conductor lasers and improved heat transfer between lasers and heat sinks. It was required that this increase in average pulse power be accomplished by an increase of energy per pulse, rather than by an increase in pulse repetition frequency. Further objective of the contract was an increase in mechanical stability of the Ga As laser device and an increased electro-mechanical correction range.

To meet the objective of the contract of an increase in average pulse power, at room temperature, IBM had proposed the use of an array of LOC heterostructure lasers in the laser device.

A technique has been developed to phase-coherently couple a monolythic array of Ga As lasers with the objective to obtain higher optical peak power of spatial coherence. In this phase-controlled mode, the far-field of the laser array is an interference pattern, containing the zero-order lobe and also higher-order grating lobes. Only when the spacings among the lasers in the array are very much smaller than the laser apertures, can most of the energy be concentrated in the zero-order lobe. (Section 3).

This requirement, however, could not be met. Using the only arrays which were available to us and which had been

diffused at IBM-FSD in Gaithersburg, prior to the contract, the intensity of each first-order grating lobe of a three laser array, was 0.25 the intensity of the zero-order lobe.

Since the array geometry could not modified, the technique of the spatially coherent beam formation was changed. A new technique was developed, that is, the spatially coherent beam formation from an array of Ga As lasers in the free running mode, where the spacings among lasers is not subjected to the same limitations as in the phase-controlled mode. In the free-running mode, the intensities of the lasers in the array are concentrated in a single Gaussian beam of spatial coherence. The far-field distribution is not influenced by the magnitude of the spacings among the lasers. In the free running mode the intersites, rather than amplitudes of the waves from the lasers in the array, are added. (Section 4).

To increase the peak pulse power, at room temperature, of the diffraction limited semi-conductor laser device, an array of three homostructure Ga As lasers was operated in the device. A spatial filter selected the spatially coherent, free running mode. The optical peak power was 5 watts, that is three times the peak power of a single laser of the dimension of the lasers in the array. The half-width of the optical pulses was 50 ns, the pulse repetition frequency 2 kHz. The synthesized far-field distribution of the three laser array is a single Gaussian beam of spatial coherence without sidelobes or grating lobes.

To extend the optical pulses in the spatially coherent mode, at room temperature, to 400 ns, as required by the contract,

heterostructure lasers should be used. Heterostructure lasers have, at room temperature, lower threshold current densities and higher differential quantum efficiencies than homostructure lasers. These improved properties are achieved primarily by confinement of the injected electrons by steps in energy.

LOC heterostructure laser material had been developed at IBM-FSD, Owego, in the previous years and could be grown with reproducable characteristics at the time of IBM's proposal. However, after IBM's proposal had been submitted to NASA-MSFC, the effort in Owego was discontinued.

To find another source for obtaining heterostructure material for the NASA contract, the Injection Laser Technology Group of IBM's Research Division was contacted. This group has developed for several years double heterostructure laser material for CW operation and had agreed to grow material for pulsed operation to the design of the project manager in IBM Gaithersburg. Though an attempt had been made to develop heterostructure material for pulsed operation at IBM Research, the effort did not succeed. The development of a new structure seems to require a larger effort than could be supported by the NASA contract.

As a alternate source, single heterostructure slivers and LOC heterostructure slivers were purchased from "Laser Diode Laboratories; Inc." in Metuchen, New Jersey. However, the purchase and tests on the heterostructure material, from "Laser Diode Laboratories" was discontinued because the characteristics of the lasers were not adequate. Also, the array geometry, made at "Laser Diode Laboratories", was not

suitable for the spatially coherent mode because of the wide spacings between the lasers in the arrays.

Though it was realized that the requirement of the contract of generating optical pulses of 400 ns duration could not be met, an attempt was made to, at least, generate optical pulses of several hundred nano-seconds in the spatially coherent mode, using homostructure lasers. To accomplish this, the heat transfer from the p-n junctions of the lasers to the large metal housing of the pulse transformer which houses the laser array, was improved. To do so, one heat sink of the laser array was soldered directly between the inner and outer conductor of the low impedance coaxial transmission line which is coupled to the pulse transformer.

Also, the pulse transformer of the laser device was modified to yield injection current pulses up to 220 Amp and 400 ns duration. This was accomplished by doubling the area of the toroidal core of the transformer and by increasing the number of turns of the primary winding from four to six.

We also have designed and assembled a pulse generator which could produce square-wave pulses of up to 60 amp, and up to 400 ns duration, with 1 ohm output impedance. This pulse generator was designed to use an "Electron Bombarded Semi-conductor" which had been purchased from Watkins-Johnson, Company". However, the driver never became operative, since the semi-conductor never functioned properly.

Because of the limitations outlined above, optical pulses of 400 ns duration in the spatially coherent mode could not

be generated. However, the energy per pulse, at room temperature, of the diffraction limited semi-conductor laser device could still be increased considerably. An array of three homostructure lasers was operated in the spatially coherent, free running mode, in the laser device. Optical pulses were generated of 5 watts at their leading edge, but the power decreased to 3.5 watts after 200 ns. Distortions in the waveform of the pulse generator can be partly responsible for the drop in optical power.

The mechanical stability of the laser device was improved by soldering one heat sink of the laser array to the transmission line which is part of the pulse transformer. Also, to facilitate the transition from mechanical alignment of the laser device to the electro-mechanical alignment control, a coupling device was inserted between each half of the optical cavity and the corresponding transducer.

The range of the electro-mechanical alignment correction was not increased because the limited rigidity of transducers with larger correction range, might adversely affect the stability of the laser device.

The laser device operating with an array of three homostructure lasers was demonstrated July 7, 1975, to Mr. J. A. Dunkin of NASA-MSFC. A photograph of the laser device is shown in Figure 2.1 and the assembly drawing is shown in Figure 2.2.

The laser device with the improved properties was delivered to Mr. J. A. Dunkin on July 10, 1975, together with an an external cylindrical lens of 21 cm focal length, and four arrays of three homostructure lasers.

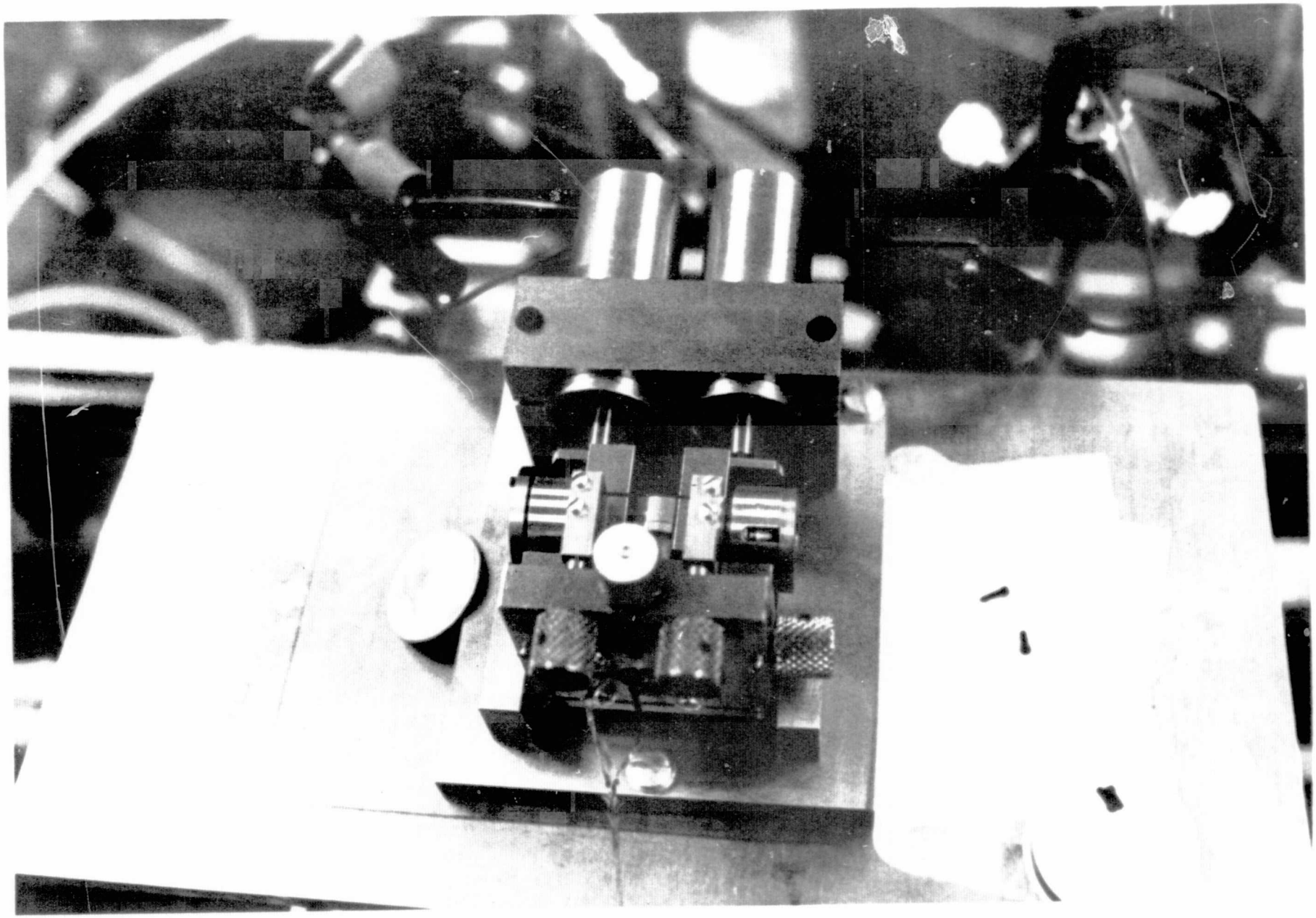

Fig. 2.1 GaAs Laser Device for Spatially Coherent Radiation at Room Temperature

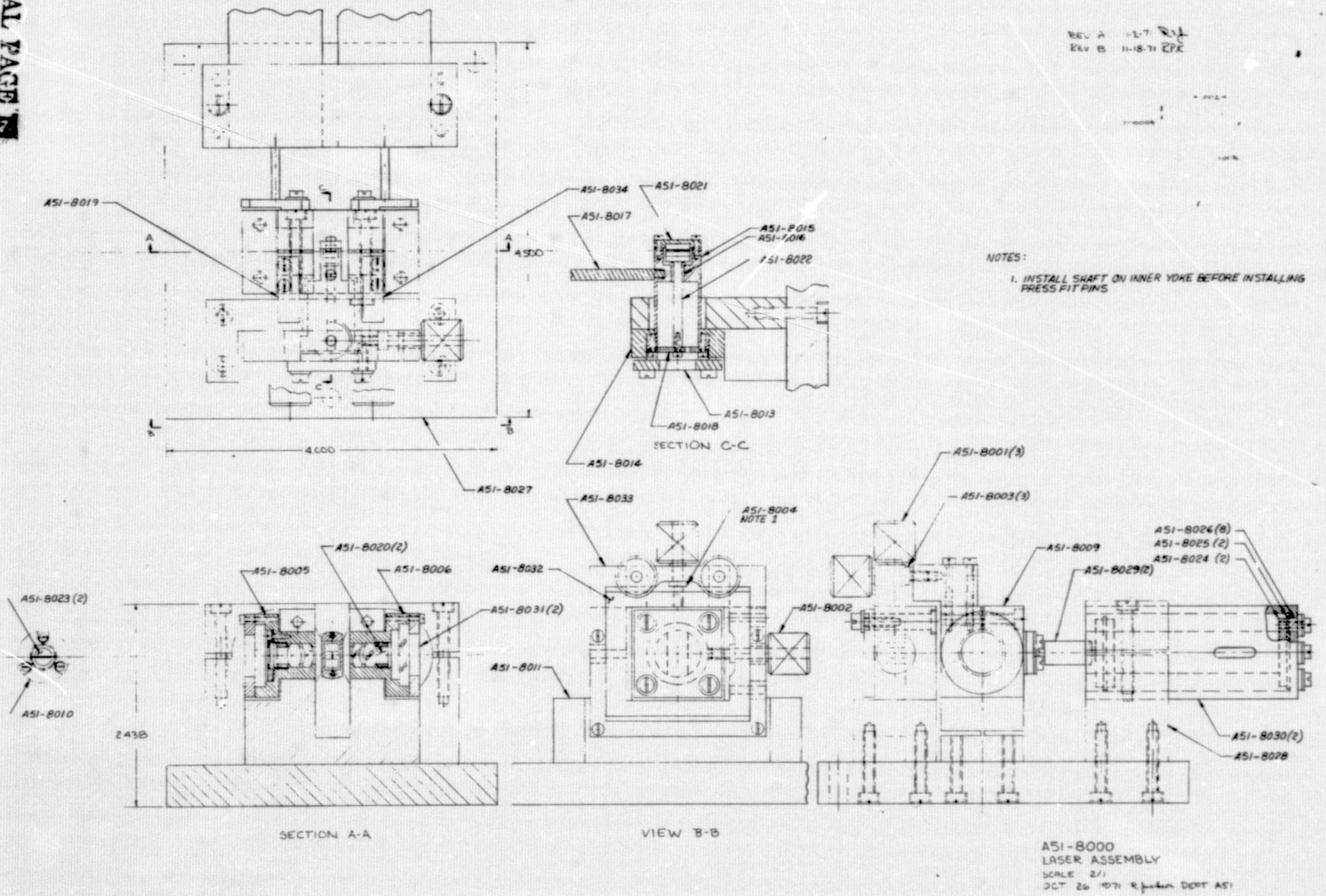

Fig. 2.2 Assembly of Laser Device

A pulse generator was also delivered to Mr. Dunkin, July 10, 1975, together with a single laser for operation in the laser device.

At the end of the contract, July 31, 1975, the Final Report and a complete set of drawings of the laser device will be send to NASA-MSFC together with a second pulse generator which yields higher energy pulses.

3. Spatially coherent radiation from an array of GaAs lasers*

Elisabeth M. Philipp-Rutz (Phase-controlled Mode)

IBM Federal Systems Division, Gaithersburg, Maryland 20760
(Received 25 November 1974; in final form 11 February 1975)

Spatially coherent radiation from a monolithic array of three homostructure GaAs lasers is reported. The three lasers, with their mirror faces antireflection coated, are operated in an external optical cavity built of spherical lenses and plane mirrors. The spatially coherent beam formation makes use of the Fourier transformation property of the internal lenses. The transverse mode control is performed by a spatial filter. The optical peak power at room temperature of the device was measured to be 5 W, three times the power of a single laser in the array. From the synthesized far-field distribution which was evaluated, we conclude that the laser radiation is of spatial coherence.

PACS numbers: 42.50., 42.60.N

Optical coupling between two adjacent stripe-geometry junction lasers has been reported, providing simultaneous coherent operation of both lasers at the same optical frequencies.[1] It has been suggested[1] that a broad source with spatial coherence could be obtained by internally coupling parallel single-filament junction lasers in a monolithic array. In this letter, phase-coherent coupling of three homostructure GaAs lasers in a monolithic array to obtain radiation of spatial coherence is reported. The three lasers (with their mirror faces antireflection coated) are operated in an external optical cavity, built of spherical lenses and plane mirrors, similar to that reported previously[2] (Fig. 1). The laser array and the plane mirrors are at the focal planes of the internal lenses of the optical cavity. The spatially coherent beam formation makes use of the Fourier transformation property of the internal lenses.[3] The transverse mode control is performed by a spatial filter which replaces the totally reflecting mirror in the optical cavity.

In designing the spatial filter, we realize that at the second focal plane of the internal lenses, the waves, set up by the fields of the lasers in the array, occupy the same space. The resultant field distribution at the second focal plane, therefore, is determined by the phase relations between these waves. The spatial filter, at the second focal plane, is matched to the interference function, which results when the fields of the lasers in the array are in the lowest-order transverse mode and when the fields are all in phase. To form the spatial filter, which selects the spatially coherent mode, the surface of the totally reflecting plane mirror is subdivided into highly reflecting strips subtending the m-order maxima in the interference function (where $m = 0$ and 1).

The field distribution at the second focal plane of the internal lenses $U(x_f, y_f)$ is the Fourier transform of the field distribution of the lasers in the array[3]; it is

$$U(x_f, y_f) \propto \exp\left[-\left(\pi \frac{w_x x_f}{\lambda_0 f}\right)^2\right] \frac{\pi \cos[(2\pi w_y/\lambda_0 f)\, y_f]}{(\frac{1}{2}\pi)^2 - [(2\pi w_y/\lambda_0 f)\, y_y]^2} \times \left\{1 + \exp\left[j\left(\frac{2\pi s}{\lambda_0 f} y_f + \varphi_1\right)\right] + \exp\left[-j\left(\frac{2\pi s}{\lambda_0 f} y_f - \varphi_2\right)\right]\right\}. \quad (1)$$

Equation (1) is valid when the array is placed symmetrically with respect to the optical axis of the cavity. The field distribution of each laser perpendicular to the junction (x_0 direction) is approximated by a Gaussian function and along the junction (y_0 direction), for the TEM_{00} mode, by a cosine function. The spot diameter of the dielectric waveguide mode is $2w_x$. The mode width of each laser along the p-n junction is $2w_y$. The center-to-center spacing between the lasers is s. The relative phase angles between the fields of the lasers are φ_1 and φ_2.

Equation (1) represents the spatial superposition of the waves at the second focal plane of the internal lenses, set up by the fields of the three lasers in the array. The waves have all the same amplitude distribution with a single maximum on the optical axis. The wave fronts of the waves at the second focal plane of the internal lenses in Eq. (1) are plane; but the wave fronts of the waves from the two lasers, which are not centered on the optical axis, are tilted with respect to the optical axis.

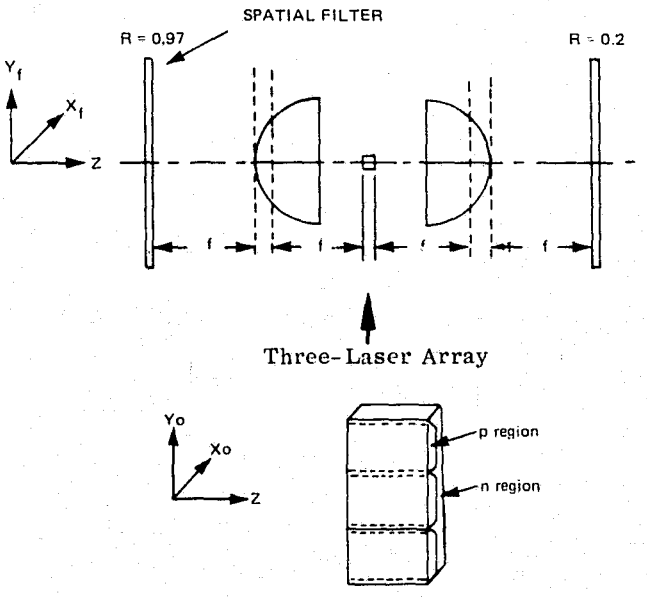

FIG. 1. GaAs laser device with three-laser array.

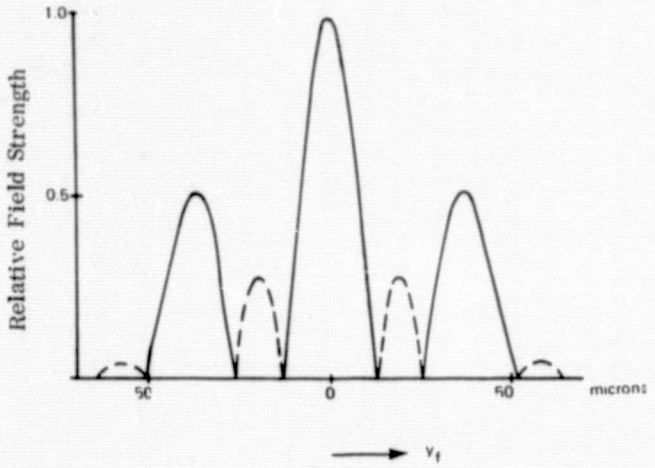

FIG. 2. Field distribution of three-laser array at second focal plane of internal lenses computed from Eq. (2). Solid lines, in-phase components. Dashed lines, out-of-phase components.

For spatial coherency, all the waves must be in phase. From Eq. (1), we derive the interference function at the second focal plane for $\varphi_1 = \varphi_2 = 0$:

$$U(x_f, y_f) \propto \exp\left[-\left(\pi \frac{w_x x_f}{\lambda_0 f}\right)^2\right] \frac{\pi \cos[(2\pi w_y/\lambda_0 f) y_f]}{(\frac{1}{2}\pi)^2 - [(2\pi w_y/\lambda_0 f) y_f]^2} \times \frac{\sin(3\pi s/\lambda_0 f) y_f)}{\sin[(\pi s/\lambda_0 f) y_f]} . \quad (2)$$

The field distribution at the second focal plane of the internal lenses, is shown in Fig. 2. It was computed from Eq. (2) for typical dimensions of our diffused GaAs lasers, where the mode width is $2w_y = 190$ μm, $s = 230$ μm, $f = 1$ cm, and $\lambda_0 = 0.9$ μm.

The spatial filter which is matched to the interference function is formed by three highly reflecting strips on a plane disk at the second focal plane of the internal lens. The three strips subtend the dominant in-phase components of the interference function; that is, the zero- and first-order grating lobes. The spatial filter reduces the photon lifetime of all higher-order transverse modes and sets up a self-reproducing field pattern where the field of each laser is in the lowest-order transverse mode and where the fields of all lasers are in phase.

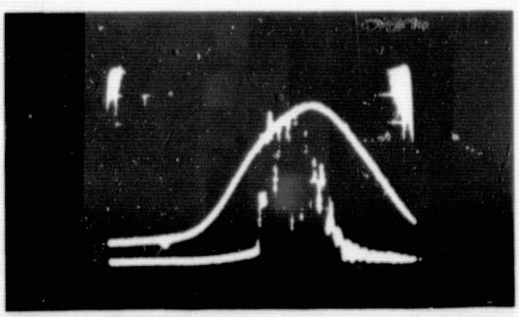

FIG. 3. Optical waveform (lower trace) and injection current (upper trace) of three-laser array in spatially coherent mode. Horizontal scale: 20 ns/div. Vertical scale: lower trace 875 mW/div; upper trace 40 A/div.

Experiments were performed using a monolithic array of three diffused homostructure GaAs lasers in the external optical cavity, shown in Fig. 1. The optical cavity is built of spherical lenses of 1-cm focal length, a plane mirror with 0.2 reflectivity, and a plane disk of fused silica with the spatial filter. The laser array, the plane output mirror, and the spatial filter are placed at the focal planes of the internal lenses.

The laser array is mounted on metal heat sinks, which provide common contacts to the lasers. The width of each laser in the array is 190 μm and the distance between laser centers is 230 μm. The mirror faces of the lasers are antireflection coated. The spatial filter which is matched to the interference function in Fig. 2 is formed by three golden strips with a reflectivity of 0.97. The strips are 25.4 μm wide and are spaced 12.7 μm apart.

The experiments were performed at room temperature, the shape of the injection current pulses was close to that of a cosine function, the pulse half-width was 100 ns, and the pulse repetition frequency was 2 kHz.

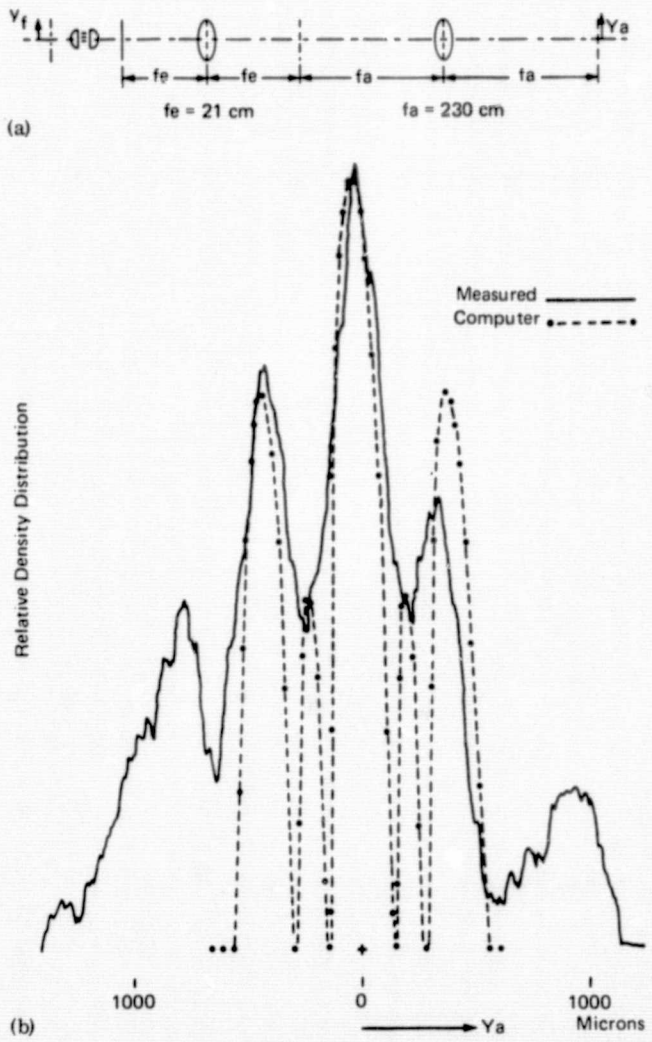

FIG. 4. (a) Beam transformation in plane of laser array. (b) Density distribution of synthesized far-field of three-laser array in plane of array.

We have measured the peak pulse power and the synthesized far-field distribution of the GaAs laser array radiating in a spatially coherent mode.

The optical peak power was detected by a calibrated ITT photodiode with an S-1 surface and displayed together with the injection current on a dual-trace Tektronic oscilloscope, type 454. The typical optical waveform is shown in Fig. 3. The optical peak power is close to 5 W. The peak injection current is approximately 180 A. The measured peak power of the three laser array is, in fact, three times the typical peak power of a single laser of the dimensions of the lasers in the array.[2]

The optical waveform shows a deep and periodic modulation which is typical for the phase-controlled mode of a GaAs laser array. The frequency of the modulation is close to that of the spiking resonance of the laser device. The deep modulation of the optical waveform seems to build up when the spiking resonance coincides with an integral multiple of the inverse round-trip time of the external cavity.

We have synthesized the far-field distribution of the laser radiation using the beam transformation shown in Fig. 4(a). The external cylindrical lens of focal length fe restores the diffraction pattern of the three-laser array in the Fraunhofer region. Its focal plane is at the second focal plane of the internal spherical lens; the curvature of the cylindrical lens is in the direction of the junctions.

The Fraunhofer region is synthesized by the external spherical lens of focal length fa. The far-field distribution was observed at the second focal plane of the external spherical lens. The other focal plane of this lens coincided with the second focal plane of the external cylindrical lens.

The synthesized Fraunhofer diffraction pattern is similar to the field distribution in Eq. (2), but magnified in the plane of the array, by the ratio fa/fe.

The evaluate the synthesized far-field distribution of the laser beam, an image was formed on a photographic plate and the density distribution of the image was then recorded using a microdensitometer. Within the linear region of the characteristic curve of the photographic plate, the density distribution of the image (D) is related to the logarithm of the intensity distribution at the second focal plane of the external spherical lens, $(U_{fa})^2$, by

$$D = \log_{10}(U_{fa})^2. \tag{3}$$

The density distribution of the synthesized far-field distribution, in the plane of the laser array, is given in Fig. 4(b). In the same figure, we also show the density distribution computed from Eq. (2), where we substitute $(fe/f)w_y$ for w_y, $(fa/fe)y_f$ for y_f, and fa for f, and from Eq. (3), for $fe = 21$ cm and $fa = 230$ cm. There is good agreement between the structure of the synthesized far-field distribution and the computed values, though the nulls in the interference function could be observed. This can be due to the nonlinearity of the photographic emulsion and to the fact that the two external lenses were not precision lenses. The high density of the nonzero-order grating lobes in Fig. 4(b) is caused by the logarithmic characteristic of the photographic emulsion. The intensity of each first-order grating lobe is 0.25, the intensity of the zero-order lobe. To concentrate more of the laser energy in the zero-order grating lobe, the spacings between the active regions of the lasers in the array must be made smaller.

The author wants to thank F. T. Byrne for helpful discussions and for reviewing the manuscript, and P. Zory and L. Comerford for implementing the spatial filter.

*Work partly supported by NASA.

[1]J. E. Ripper and T. L. Paoli, Appl. Phys. Lett. **17**, 371 (1970).
[2]E. M. Philipp-Rutz, IEEE J. Quantum Electron. **QE-8**, 632 (1972).
[3]J. W. Goodman, *Introduction to Fourier Optics* (McGraw-Hill, New York, 1968).

4. SINGLE LASER BEAM OF SPATIAL COHERENCE FROM AN ARRAY OF GaAs LASERS * (FREE RUNNING MODE)

Abstract: Spatially coherent radiation from a monolythic array of three GaAs lasers in a free-running mode is reported. The lasers with their mirror faces anti-reflection coated, are operated in an external optical cavity, built of spherical lenses and plane mirrors. The spatially coherent beam formation makes use of the Fourier transformation property of the internal lenses. The transverse mode control is accomplished by a spatial filter.

The optical cavity is similar to that used for the phase-controlled mode of spatially coherent beam formation, which had been reported; only the spatial filters are different. The spatial filter in the free-running mode controls the fields of the lasers to be in the lowest-order transverse mode, but it does not control their phase angles. Random amplitude and phase variations of the longitudinal modes prevent the formation of a stationary interference waveform. In the far-field (when restored by an external lens), the intensities of the lasers in the array are concentrated in a single laser beam of spatial coherence, without any grating lobes. The far-field distribution is not influenced by the spacings among the lasers. The far-field distribution of the laser array in the free-running mode differs significantly from the interference pattern of the phase-controlled mode.

The modulation characteristics of the optical waveforms of the two modes are also quite different. This is because the modulation is related to the interaction of the spatial filter with the longitudinal modes of the laser array with the optical cavity. The modulation of the optical waveform of the free-running mode is nonperiodic, confirming that the fluctuations of the optical fields of the lasers are random.

Experiments were performed at room temperature using a monolythic array of three GaAs lasers. The far-field distribution of the laser array and the optical waveform were investigated.

* Will be published in October 1975 issue of the Journal of Applied Physics

4.1. INTRODUCTION

A technique has been reported to phase-coherently couple a monolythic array of GaAs lasers with the objective to obtain higher optical power of spatial coherence.[1,2] In this phase-controlled mode, the far-field of the laser array (when restored by an external lens) is an interference pattern, containing the zero order lobe and also higher order grating lobes. Only when the spacings among the lasers in the array are very much smaller than the laser apertures, can most of the energy be concentrated in the zero-order lobe.

In this paper, a free-running mode of spatially coherent beam formation from an array of GaAs lasers, is reported, where the spacings among lasers is not subjected to the same limitations as in the phase-controlled mode. In the free-running mode, the intensities of the lasers in the array are concentrated in a single beam of spatial coherence. The far-field distribution is not influenced by the magnitude of the spacings among the lasers.

The GaAs laser array, in the free-running mode, is operated with an external optical cavity built of spherical lenses and plane mirrors, which is similar to that used for the phase-controlled mode.[1,2] The laser array and the plane mirrors are at the focal planes of the internal lenses of the optical cavity. The spatially coherent beam formation makes use of the Fourier transform property of the internal lenses[3]; it is performed by a spatial filter which replaces the totally reflecting mirror in the optical cavity.

The spatial filter of the free-running mode is different from that in the phase-controlled mode. The spatial filter in the free-running mode, not only selects a far-field distribution which is different from that of the phase-controlled mode, but also interacts differently with the longitudinal modes of the GaAs laser array with the optical cavity.

The different interactions are evaluated and related to the different modulations of the optical waveforms of the two modes.

Experiments were performed at room temperature using a monolythic array of three GaAs lasers. Experimental results on the peak pulse power, the optical waveform, and the synthesized far-field distribution of the three laser array in the free-running mode are presented.

4.2. SPATIALLY COHERENT BEAM FORMATION

The technique of spatially coherent beam formation of an array of GaAs lasers makes use of the Fourier transform properties of the lenses in the external optical cavity in Figure 1. The optical cavity is built of spherical lenses and plane mirrors. The lasers in the array (with their mirror faces anti-reflection coated) and the plane mirrors, are at the focal planes of the internal lenses. The spatial filter is implemented by reducing the width of the totally reflecting mirror.

To describe the spatially coherent beam formation, the Fourier transformation of the waves from an array of three lasers, radiating in the lowest order transverse mode, will be computed. The lasers in the array are placed symmetrically in respect to the optical axis of the cavity. For the computations we have approximated the field of each laser perpendicular to the junction (x_o - direction) by a Gaussian function, and the field along the junction (y_o - direction) of the TEM_{oo} - mode, by a cosine function. The spot diameter of the dielectric waveguide mode is $2w_x$. The mode width of each laser diode along the p-n junction is $2w_y$. The center-to-center spacing between the lasers is s. The instantaneous amplitude and phase angle of the field of each laser are $a_m(t)$ and $\varphi_m(t)$, for m = 1,2,3. Amplitude and phase angle are slowly varying with time, the variations are random[4].

The transformation of the fields of the lasers in the array from one focal plane of the lenses (with the focal length f), to the second focal plane, yields the distribution:

$$u(x_f, y_f) \sim \int_{-\infty}^{+\infty} e^{-\left(\frac{x_o}{w_x}\right)^2} \left(a_1(t)\, e^{j\varphi_1(t)} \int_{-(s+w_y)}^{-(s-w_y)} \cos\left(\frac{\pi}{2w_y}(y_o+s)\right) + a_2(t)\, e^{j\varphi_2(t)} \int_{-w_y}^{w_y} \cos\left(\frac{\pi}{2w_y} y_o\right) + a_3(t)\, e^{j\varphi_3(t)} \int_{s-w_y}^{s+w_y} \cos\left(\frac{\pi}{2w_y}(y_o-s)\right) \right) \cdot e^{j\frac{2\pi}{\lambda f}(x_o x_f + y_o y_f)}\, dx_o\, dy_o \qquad (1)$$

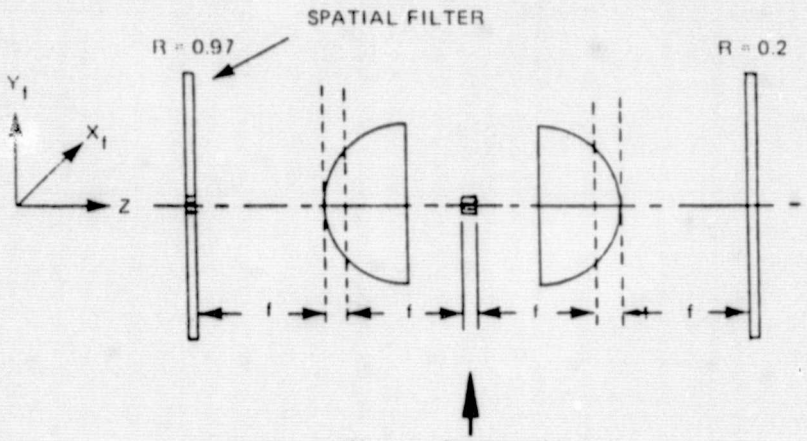

Three-Laser Array

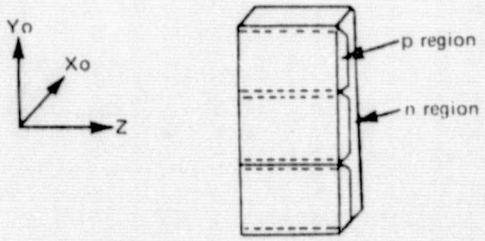

Three-Laser Array

Figure 1. GaAs Laser Device with Three-Laser Array

$$u(x_f, y_f) \sim e^{-\left(\pi \frac{w_x x_f}{\lambda f}\right)^2} \frac{\pi \cos\left(\frac{2\pi w_y}{\lambda f} y_f\right)}{\left(\frac{\pi}{2}\right)^2 - \left(\frac{2\pi w_y}{\lambda f} y_f\right)^2}$$

$$\left(a_1(t)\, e^{j\left(\frac{2\pi s}{\lambda f} y_f + \varphi_1(t)\right)} + a_2(t)\, e^{j\varphi_2(t)}\right.$$

$$\left. + a_3(t)\, e^{-j\left(\frac{2\pi s}{\lambda f} y_f - \varphi_3(t)\right)}\right) \qquad (2)$$

The field at the second focal plane of the lenses in Equation 2, is the spatial superposition of the waves which were set up by the fields of the three lasers in the array. The waves have all the same spatial amplitude distribution with a single maximum on the optical axis. The wavefronts of the waves at the second focal plane of the internal lenses are plane, but the wavefronts of the waves from the two lasers which are not centered on the optical axis, are tilted in respect to the normal to the optical axis by the angles $\pm\Theta$, which are

$$\pm \Theta = \pm \arcsin \frac{s}{f} \qquad (3)$$

The waves impinging on the plane mirrors of the optical cavity are partly reflected. The waves from the outer lasers, because of their conjugate tilt-angles, are reflected towards the symmetrically placed lasers, setting up two counter circulating waves, similar to those in a ring laser.[5]

To select the free-running mode, the photon lifetime of this mode must be higher than that of any other mode. To accomplish this, a spatial filter must be placed at the second plane of one or both lenses in the optical cavity, where the waves from the three lasers are spatially superimposed. The spatial filter in the free-running mode controls the field of each laser in the array to be in the lowest order transverse mode, but it does not control their phase angles. The spatial filter is implemented by reducing the width of the totally reflecting mirror to form a highly reflecting strip. The strip subtends the spatial field distribution in Eq. 2. The spatial filter reduces the photon lifetime of all transverse modes in the three lasers with the exception of the lowest order transverse mode.

The far-field distribution of the laser array when restored by an external lens, is the magnified field distribution at the output mirror of the optical cavity, where the waves from the three lasers are spatially superimposed. To derive the interaction of the superimposed waves, the time dependence of the optical fields of the lasers in the array, was evaluated.

In the free-running mode of the GaAs laser array, the spatial filter does not exert any control on the longitudinal modes of the laser array with the optical cavity. Without control, the amplitudes and phase angles of the longitudinal modes are slowly varying with time; these variations are random. The instantaneous optical field of each laser can be described in the general form:

$$u(t) = \sum_{n=-N}^{+N} a_n(t)\, e^{j(\omega_n t + \varphi_n(t))} \qquad (4)$$

where $a_n(t), \omega_n$ and $\varphi_n(t)$ are the real amplitude, the frequency and the phase of the n-th longitudinal mode. The frequencies of these modes are separated by Ω, where $\Omega = \frac{2\pi}{T}$, and T is the round-trip time in the optical cavity. The fluctuations of the optical field resulting from the summation of randomly phased monochromatic waves with randomly varying amplitudes, are completely random. The duration

T_{coh} of the most rapid fluctuations is the inverse of the oscillating bandwidth $\Delta\bar{\nu}$ of the laser radiation.[4] (For the spatially coherent GaAs laser array $\Delta\bar{\nu} \approx 15\text{Å}$ and $T_{coh} \approx 2 \times 10^{-12}$s).

Equations 1 and 2 were derived for the lasers in the array oscillating in a single longitudinal mode. But they are equally valid for each of the many longitudinal modes of the GaAs laser array with the optical cavity. To evaluate the temporal variations of the optical fields of the lasers in the array, each term in Equation 2 must be replaced by the summation over all the longitudinal modes, similar to that in Equation 4. It follows that the optical field of each laser in the array fluctuates randomly. These random fluctuations prevent the formation of a stationary interference pattern and the intensitites, rather than the amplitudes of the waves from the lasers in the array, are added.

The field distribution at the output mirror of the optical cavity (in the plane of the array) is shown in Figure 2 for typical dimensions of our diffused GaAs lasers of $2\bar{w}_y$ = 190 microns, s = 230 microns and for f = 1 cm and λ = 0.9 microns. It has a single maximum and no additional lobes. The laser beam is not diffraction limited but the radiation is in the lowest order transverse mode. The far-field distribution of the free running mode is not influenced by the magnitude of the spacings among lasers in the array.

For comparison, the field distribution at the output mirror is also shown in Figure 2 for the phase controlled mode. In this mode, the spatial filter not only constrains the fields of the lasers in the array to be in the lowest order transverse mode, but also accomplishes that they are all in phase.[1,2] The far-field, when restored by an external lens, is an interference pattern which contains, in addition to the zero-order lobe, also the first order lobes.

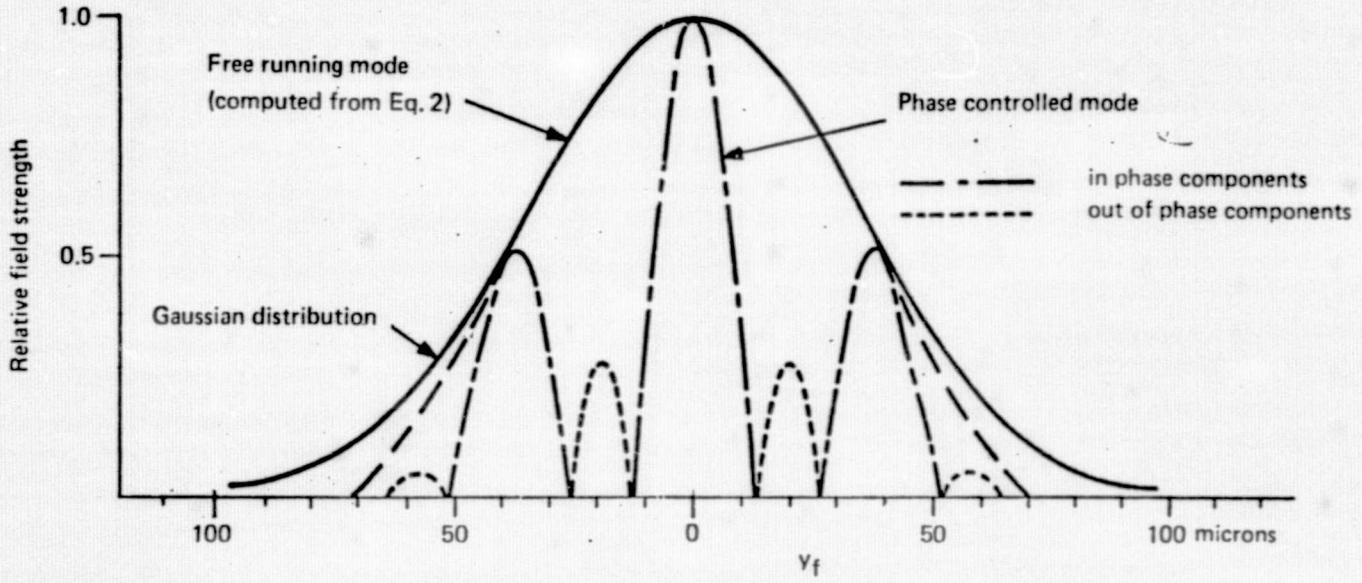

Figure 2. Field Distribution of Three-Laser Array, at Second Focal Plane of Internal Lenses;

A. For the Free Running Mode, Computed from Equation 2 (and for comparison, for a Gaussian Field Distribution)

B. For the Phase Controlled Mode.

To ascertain whether the free running mode of spatially coherent beam formation could be attained, we have measured the far-field distribution of the three laser array in the free running mode and have compared it with that of the array in the phase controlled mode.[1,2] Experimental results on the beam formation in the free running mode (Section 4) confirm that we can obtain from an array of lasers, radiation of spatial coherence in a single beam with no additional lobes. The far-field distribution of the array in the free running mode differs significantly from the interference pattern of the phase controlled mode.

4.3. TIME DEPENDENCE OF OPTICAL POWER (A Comparison with the Phase Controlled Mode)

Not only the far-field distribution is different in the two modes of spatially coherent beam formation, but also the time dependence of the optical power. This is because the optical waveforms respond to the interactions of the spatial filters with the longitudinal modes of the laser array with the optical cavity. The optical waveforms in both modes are modulated. While the modulation in the phase controlled mode is deep and periodic,[1,2] the modulation in the free running mode is neither (Section 4).

The modulations on the optical waveforms which we observe, seem to be introduced by the spiking fluctuations of the GaAs laser array with the optical cavity.[6] The spiking fluctuations are damped oscillations which result from the dynamic instability in the interaction between the inverted electron population and the optical field. In the free running mode where the spatial filter does not control the amplitudes and phase angles of the longitudinal modes, and the optical field fluctuations are random, there cannot be a periodic excitation of the spiking resonance. The modulation of the optical waveform which we observe must result from the super-position of the spiking fluctuations of the three lasers in the array which are damped and random. (The fluctuations of the optical fields could not be detected, because the oscilloscope, which was used, could not respond to the very short pulses.)

In the phase controlled mode of the laser array, the spatial filter in the optical cavity not only selects the spatial coherence of the laser radiation, it also controls the temporal variations of the optical fields of the lasers. To set-up the mode with the longest photon life time, that is, to form the stationary interference waveform to which the spatial

filter is matched, requires, that the field fluctuations of the lasers be in synchronism. To accomplish this, the spatial filter in the optical cavity must exert a control on the amplitudes and phase angles of the longitudinal modes. To synchronize the field fluctuations in the lasers, the spatial filter must constrain the amplitudes and phase angles of each of the longitudinal modes, and also the statistical phase variations among the longitudinal modes, to be the same in the lasers of the arrays. To do so, the spatial filter must also eliminate the random amplitude and phase variations with time of the longitudinal modes.

A mathematical model of the time dependence of lasers which radiate in a multitude of longitudinal modes, has been derived, where the slowly varying amplitudes and phase angles of the longitudinal modes are assumed to be constant during the emission.[4] The model shows that the statistical phase variations among the longitudinal modes yield instantaneous field fluctuations which are random but very pronounced. They are short pulses of the shape of the mode-locked pulses. But instead of one mode-locked pulse (with the duration T_{coh}) within the repetition time T, many short pulses occur. The field fluctuations in form of these short pulses are periodic in time T because of the constant difference frequency between the longitudinal modes.

We assume that, in the phase controlled mode, the field fluctuations of the lasers become periodic in time as predicted from the mathematical model. The periodic field fluctuations then excite the spiking resonance of the lasers in the optical cavity. This periodic excitation counter acts the damping of the spiking resonance and produces the deep modulation of the optical waveform. The field fluctuations of the lasers in the array which are synchronized by the spatial filter, set-up the synchronized periodic fluctuations at the spiking resonance, which we have observed.

Because the repetition time of the field fluctuations T ($T \approx 0.3$ ns) is much shorter that the period of the spiking resonance ($\frac{1}{f_s} \approx 6.7$ ns), we must assume that harmonic interaction occurs between the field fluctuations

and the spiking resonance. The deep modulation of the optical waveform seems to build up when the spiking resonance coincides with an integral multiple of the inverse of the repetition time T.

We conclude that the different modulation characteristics of the optical waveforms of the two modes of spatially coherent beam formation, reveal the difference in their temporal optical field variations. The absence of a deep and periodic modulation on the optical waveform of the free running mode confirms our assumption that the fluctuations of the optical fields with time of the lasers in the array, are random. They will prevent the formation of a stationary interference pattern in the far-field of the laser array.

4.4. EXPERIMENTAL RESULTS

Experiments were performed using a monolythic array of diffused homostructure GaAs laser diodes in the external optical cavity. The width of each laser in the array is 190 microns and the distance between laser centers is 230 microns. The mirror faces of the lasers are anti-reflection coated. The laser array is mounted on metal heat sinks which provide common contacts to the lasers. The preparation of the laser diodes has been reported previously.[6]

The external optical cavity is built of spherical lenses of 1 cm focal length and plane mirrors (shown in Figure 4.1) The laser array, the plane output mirror and the spatial filter are placed at the focal planes of the internal lenses. The reflectivity of the output mirror is 0.2. The spatial filter which selects the free running mode is formed by a gold strip on a plane disk of fused silica. In the plane of the array the strip is 127 microns wide.

We have measured the peak pulse power of the GaAs laser array, the optical waveform, and the synthesized far-field distribution. The experiments were performed at room temperature, the shape of the injection current pulses was close to that of a cosine function, the pulse half-width was 100 ns and the pulse repetition frequency was 2 kHz.

The optical peak power was detected by a calibrated ITT photodiode with an S-1 surface and displayed together with the injection current on a dual-trace Tektronic oscilloscope, type 454.

We have investigated the far-field distribution of the laser arrays using the beam transformation shown in Figure 3. The external cylindrical lens with the focal length f_e restores the diffraction pattern of the laser array in the Fraunhofer region. Its focal plane is at the second focal plane of the internal spherical lens, the curvature of the cylindrical lens is in direction of the junctions.

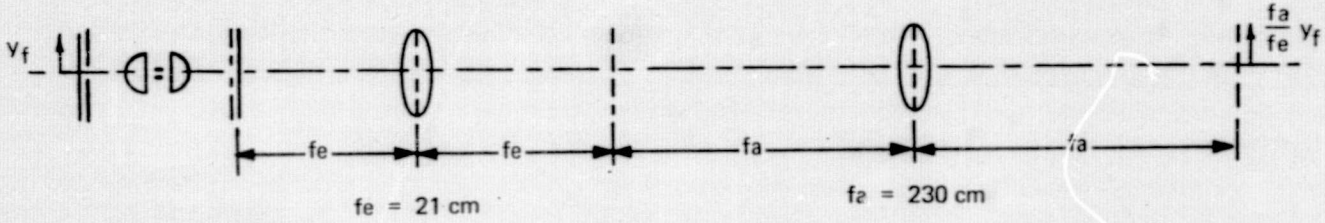

Figure 3. Beam Transformation in Plane of Laser Array

The far-field distribution itself would not be evaluated because the requirement for the validity of the Fraunhofer approximation could not be met in our laboratory. Instead, we have synthesized the Fraunhofer diffraction by the external spherical lens with the focal length f_a. One focal plane of this lens coincided with the second focal plane of the external cylindrical lens. The synthesized far-field distribution was observed at the second focal plane of the external spherical lens. The synthesized far-field distribution is similar to the field distribution at the output mirror of the optical cavity, but magnified in the plane of the junctions by the ratio $\frac{fa}{fe}$.

To evaluate the synthesized far-field distribution of the laser radiation, an image was formed on a photographic plate and the density distribution of the image was then recorded using a microdensitometer. Within the linear region of the characteristic curve of the photographic emulsion, the density distribution of the image (D) is related to the logarithm of the intensity distribution $(U_{fa})^2$ across the laser beam, it is

$$D = \log_{10} (U_{fa})^2 \qquad (5)$$

The optical peak pulse power of the three laser array in the spatially coherent, free running mode is close to 5 watts. The peak injection current is approximately 180A (Figure 4). The measured peak power is, in fact, three times the typical peak power of a single laser of the dimensions of the lasers in the array.[6]

The density distribution of the synthesized far-field distribution in the plane of the junctions of the three laser array in the free running mode is shown in Figure 5. In the same figure we also give the density distribution computed from Equation 2 where we have substituted $\frac{fe}{f} w_y$ for w_y, $\frac{fa}{fe} y_f$ for y_f and fa for f, and from Equation 5, for fe = 21 cm and fa = 230 cm. We observe that the synthesized far-field has a single maximum and no additional lobes. The recorded distribution is in good agreement with the computed function.

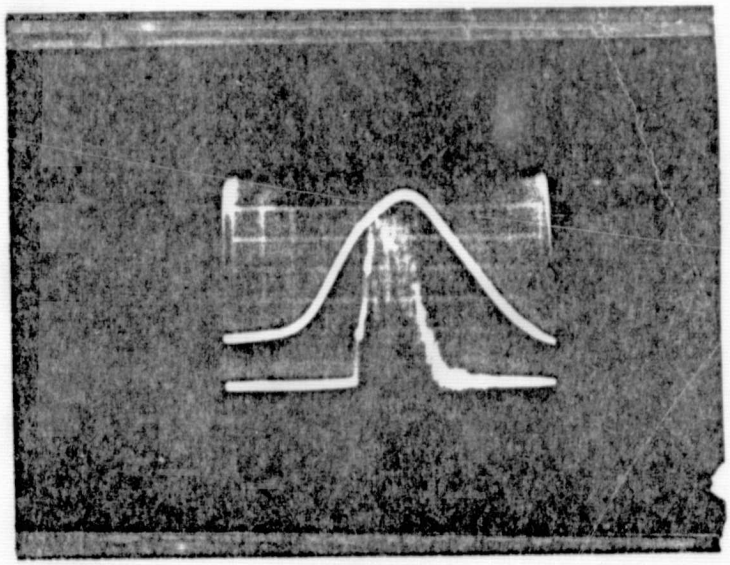

Upper vertical trace: 40 A/div
Lower vertical trace: 0.875 W/div
Horizontal trace: 20 ns/div

Fig. 6 Optical waveform (lower trace) and injection current (Upper trace) of three laser array in spatially coherent, free running mode

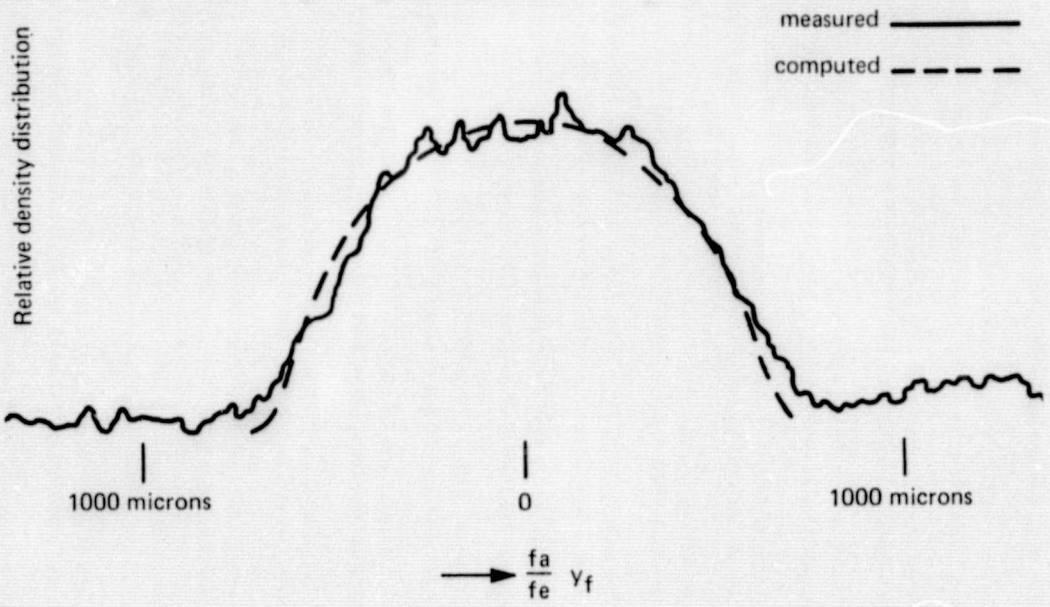

Figure 7. Density Distribution of Synthesized Far-Field of Three-Laser Array (in Plane of Array) in the Free Running Mode

The modulation of the optical waveform in Figure 4 is not periodic; it seems to result from the super-position of the spiking fluctuations of each of the three lasers in the external optical cavity, which were reported previously. (6)

Since the synthesized far-field distribution of the three laser array in the free running mode is also that of a single laser in the lowest order transverse mode, it seemed important to ascertain whether the waves from all three lasers in the array have contributed to the beam pattern in Figure 5. To do so, the spatial intensity distribution was also investigated in the region between the external spherical lens and its second focal plane. In this region, we always observe three separate beams of similar radiance, corresponding to the waves from the three lasers in the array.

The equivalence of the synthesized far-field distribution at the second focal plane of the external spherical lens, and the far-field distribution in the Fraunhofer region, is quite understandable for the phase controlled mode, since the optical field vectors of the two off-axis lasers yield a resultant vector along the optical axis. The same equivalence for the free running mode, that is the evolution from the three laser beams, at the second focal plane of the external cylindrical lens, to the formation of a single radiation maximum in the far-field, is difficult to visualize and requires examination.

The solution of the integral governing Fraunhofer diffraction, (7) evaluated at the distance z, is

$$u(x_z, y_z) \propto e^{-\left(\frac{x_z f}{\omega_x z}\right)^2} \frac{\pi \cos\left(\frac{2\pi}{\lambda} \frac{fe}{f} \frac{\omega_y}{z} y_z\right)}{\left(\frac{\pi}{2}\right)^2 - \left(\frac{2\pi}{\lambda} \frac{fe}{f} \frac{\omega_y}{z} y_z\right)^2}$$

$$\times \left(a_1(t)\, e^{j\left(\frac{2\pi}{\lambda} \frac{fe}{f} \frac{s}{z} y_z + \varphi_1(t)\right)} + a_2(t)\, e^{j\varphi_2(t)} \right.$$

$$\left. + a_3(t)\, e^{-j\left(\frac{2\pi}{\lambda} \frac{fe}{f} \frac{s}{z} y_z - \varphi_3(t)\right)} \right) \qquad (6)$$

Equation 6 represents the spatial superposition of the waves from the three lasers, where the propagation paths of the two off-axis lasers are tilted with respect to the normal to the optical axis of the cavity, by the angles:

$$\pm \Theta_e = \pm \text{ arc sine } \frac{f_e s}{f z} \qquad (7)$$

In the far-field, where z approaches infinity, the angles $\pm \Theta_e$ decrease to zero.

Actually, the spatially coherent waves from the three lasers in the array propagate from the second focal plane of the external cylindrical lens, with their propagation paths parallel to the optical axis. The waves expand as they propagate in space but their maxima remain stationary, spaced at a distance $\frac{f_e}{f}s$ apart. In the far-field, where the wave expansion by far exceeds the spacing between the radiation maxima, the three beams seem to coincide.

4. 5. CONCLUSION

Spatially coherent radiation from an array of three GaAs lasers in a monolythic array in the free running mode was obtained. In this mode, the far-field results from the summation of the intensitities of the three lasers. The far-field distribution has a single radiation maximum and no additional lobes. The radiation in the free running mode is in the lowest order transverse mode, but the laser beam is not diffraction limited.

The peak pulse power, at room temperature, is close to 5 watts.

The technique of spatially coherent beam formation which we have developed, is not limited to a three laser array, but can be extended to arrays with more lasers. We assume that, for the free running mode, it is not required that the lasers in the array are of exactly the same length.

ACKNOWLEDGEMENT

The author wants to thank F. T. Byrne, A. W. Smith, and P. Zory for helpful discussions and A. W. Smith and F. T. Byrne for reviewing the manuscript, also P. Zory and L. Comerford for implementing the spatial filter.

References

1. Philipp-Rutz, E. M., 1974 IEEE Int. Semiconductor Laser Conference, Atlanta, Georgia, Nov. 1974

2. Philipp-Rutz, E. M., Appl. Phys. Letters, 26, 475 (1975)

3. J. W. Goodman, Introduction to Fourier Optics, McGraw-Hill Book Co. (1968)

4. A. A. Grutter, H. P. Weber and R. Dandliker, Phys. Review, 185, 629 (1969)

5. N. Buholz and M. Chodorow, IEEE J. Quantum Electr., QE-3, 454 (1967)

6. Philipp-Rutz, E. M., IEEE, Quantum Electr., QE-8, 632 (1972)

7. M. Born and E. Wolf, Principles of Optics, Pergamon Press, 1964-65.

5. Relation Between Periodic Modulation in Optical Waveform and Mode-Locking

To optimize the optical peak power in the spatially coherent, free running mode, of the three laser arrays, the distance between the internal lenses and the plane mirrors in the optical cavity was adjusted until a periodic modulation in time of the optical waveform, was observed. This modulation which is shown in Fig. 5.1, seems to result from the interaction of the two outer lasers in the array, which form a ring laser. It seemed important to ascertain whether the periodic modulation in the optical waveform could possibly indicate a conversion of the free running mode to the phase-controlled mode.

For this investigation a two laser array was used where the two lasers in the array form the ring laser. It was a two laser array of the material 15/56, with 300 microns junction width. The transverse mode control was accomplished by a gold strip of 110 microns width in or close to the focal plane of the internal lens of the optical cavity. The gold strip subtends the entire field of the TEM_{00} - mode, while it discriminates against the TEM_{01} -mode, which extends over a width of 240 microns. These field distributions were not measured but derived from linear theory of beam transformation. They do not take beam distortions by the non-linear characteristics of the laser medium into consideration.

For higher optical power the output mirror was moved from the focal plane of the internal lens, towards the lens, by approximately 0.2 mm, and the gold strip was moved from the focal plane towards the lens by approximately 0.55 mm. At this position the optical waveform is strongly modulated, as shown in Fig. 5.2; the peak pulse power was close to 4 watts. However, the

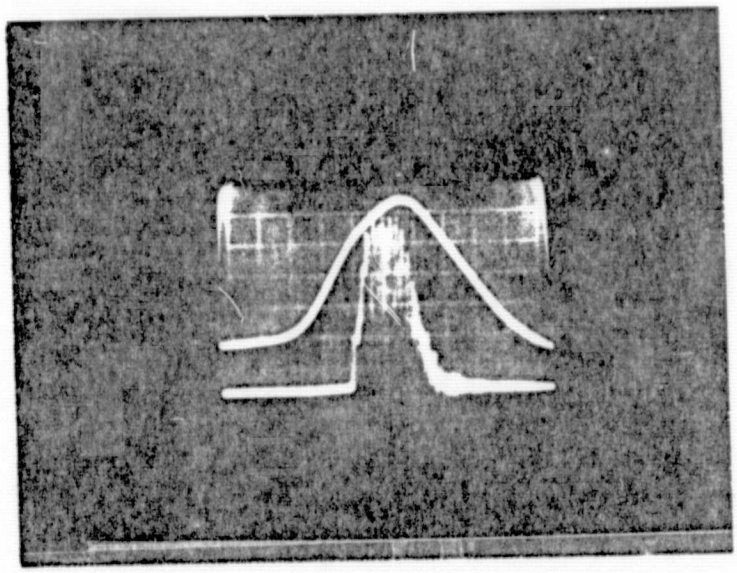

Upper vertical trace: 40 A/div

Lower vertical trace: 0.875W/div

Horizontal trace: 20 ns/div

Fig. 5-1 Injection current and optical waveform of three laser array, in the spatially coherent, free running mode. Spatial filter: 127 microns

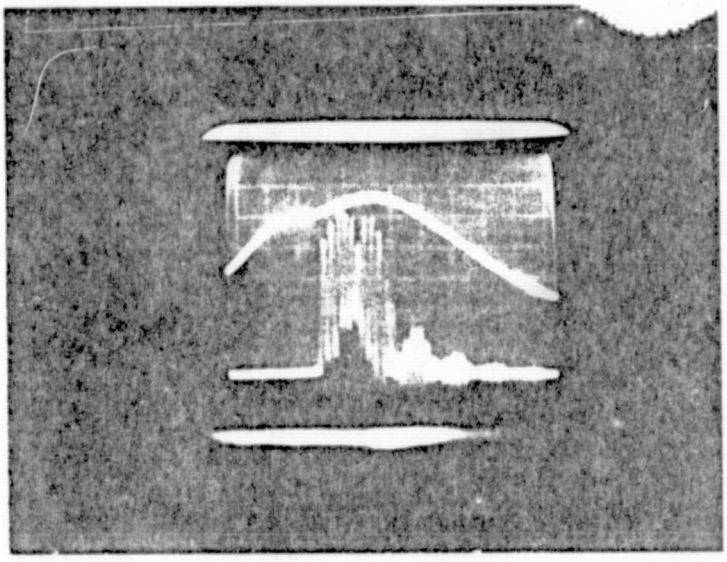

Upper vertical trace: 60 A/div

Lower vertical trace: 1 W/div

Horizontal trace: 20 ns/div

Fig. 5-2 Injection current and optical waveform of two laser array in spatially coherent, free running mode. Spatial filter: 110 microns

synthesized far-field distribution of the laser array is that of the spatially coherent, free running mode, as shown in Figs 5.3 and 5.4, where microdensitometer traces of the synthesized far-field distribution are shown, for different magnifications. In the same figures, values computed for the density distribution of the synthesized far-field of the spatially coherent beam in the free running mode, are also given. There is good agreement between measured and computed distributions.

We also observe in Figure 5.3 that no spatial modulation of the laser fields seems to occur. (In the synthesized far-field, the spatial modulation of the laser fields would appear in form of a pair of modulation sidebands which are spaced approximately $\pm$ 6mm from the main beam. These sidebands, if present, can be eliminated by a slit at the output mirror of approximately 800 microns width).

The deep periodic modulation of the optical waveform of the spatially coherent radiation of the two laser array in Figure 5.2 is close to the rate of the spiking resonance of the Ga As lasers in the external optical cavity. From the fact that modulation is not damped, we conclude that the spiking resonance is excited by periodic intensity fluctuations. The periodic intensity fluctuations in the two lasers, which form the ring laser, seem to be coupled, such that the spiking resonances in both lasers become synchronized.

In a gas ring laser spontaneous mode-locking in the absence of applied moduation, had been reported. This type of spontaneous mode-locking, which depended on cavity length and position of the

5-5

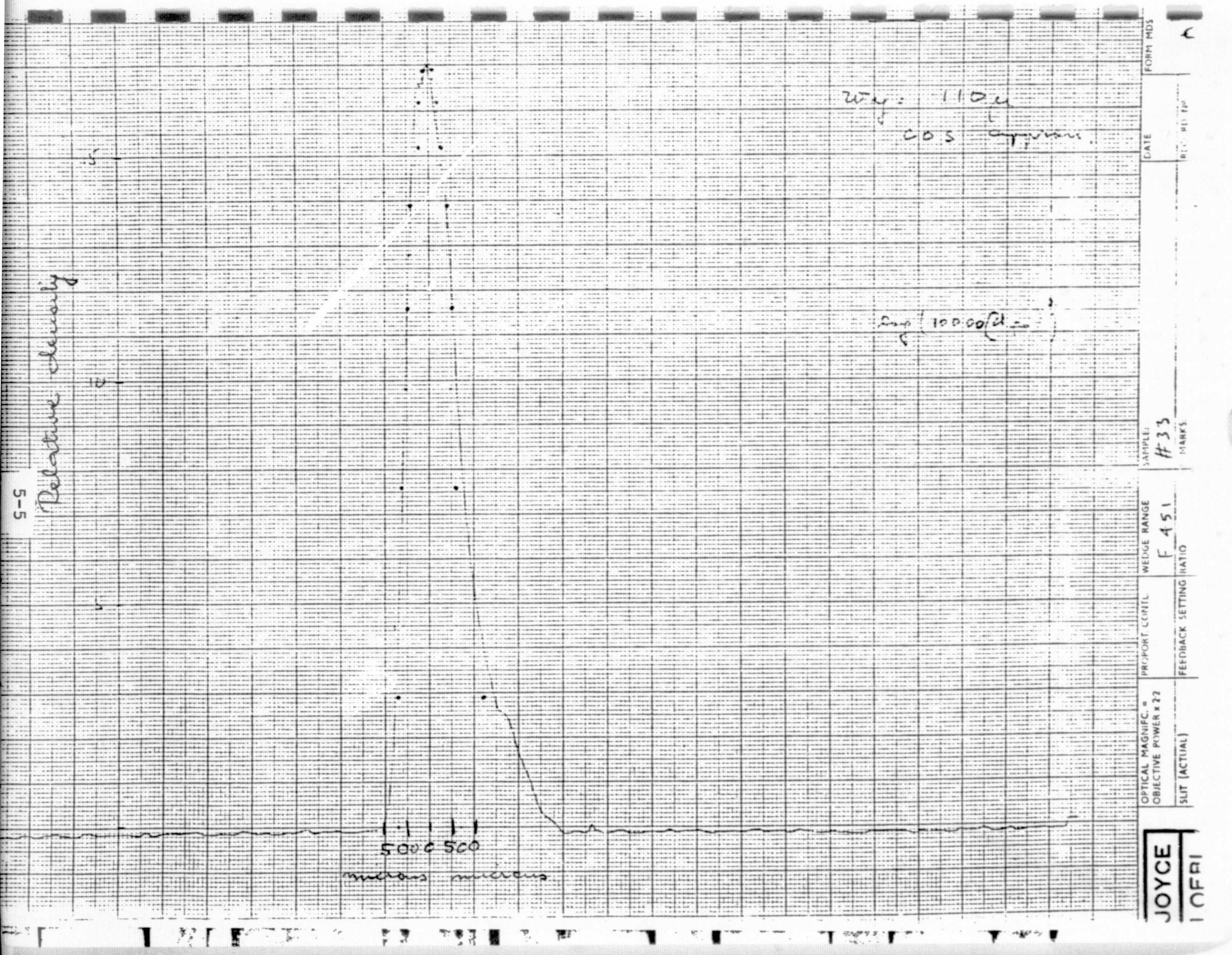
Relative density
5000 500
microns microns
#33
F 451
SAMPLE
MARKS
WEDGE RANGE
RATIO
PROPORT. CONTL.
FEEDBACK SETTING
OPTICAL MAGNIFC. = OBJECTIVE POWER x 22
SLIT (ACTUAL)
DATE
FORM MDS
JOYCE
LOEBL

Relative density
1
.5
.1
.05
1000
500
0
500
1000
microns
10 log (100(μ Pa)²)
JOYCE
OPTICAL MAGNIFC. =
OBJECTIVE POWER = 22
PROPORT. CONTL.
WEDGE RANGE
SAMPLE:
#32 D1
DATE
FORM
DS

5-6

FIG. 5

laser medium in the cavity, more than one locked pulse within the cavity round trip time, was observed. Specifically, the cavity contained two equally spaced clockwise circulating pulses and two equally spaced counter-clockwise pulses. In all instances where mode-locking was observed, the laser medium was located at a region in the cavity where it was exposed alternately to left traveling and right traveling pulses. The mode-locked pulses remained symmetrically timed with respect to the active medium. The symmetrical timing yields the longest intervals between counter rotating pulses to build-up the inverted electron polulation which had been depleted by the previous pulse.

The periodic modulation in time of the optical waveform of the laser array can possibly be explained by mode-locking of the intensity pulsations in the Ga As lasersin the array. This explanation made it necessary to carefully examine the far-field of the two laser array in the free running mode.

Symmetrically timed mode-locked pulses in the Ga As laser array with the external optical cavity, when traveling in opposite direction, will cross at the plane mirrors of the optical cavity when an odd number of mode-locked pulses are present; but they will not cross at the mirrors when an even number of mode-locked pulses is generated. Simultaneous arrival of the circulating and counter-circulating mode-locked pulses at the output mirror, will result in the setting up of an interference pattern similar to that observed in the phase-controlled mode.

The synthesized far-field distribution in Figures 5.3 and 5.4, however, does not indicate any interference of the counter circulating pulses. However, it seems unlikely that always

an even number of mode-locked pulses is generated, since there is no mechanism which prefers even numbers of mode-locked pulses.

Crossing of the mode-locked pulses at the plane mirrors can also be prevented when the circulating and counter-circulating pulses are not timed symmetrically. Symmetrical timing requires that the oppositely directed pulses are of the same intensity such that they deplete the inverted electron population by the same amount, and the same time interval is required to again build up the inverted population. However, a slight asymmetry in the ring laser will set-up competition effects of the oppositely directed pulses, with the result that the intensities of the mode-locked pulses, traveling in one direction, are higher than those traveling in the opposite direction. In that case, the oppositely directed mode-locked pulses will not be symmetrically timed any longer. The time interval between the larger pulse traveling through the active medium and the smaller pulse traveling through the same active medium, but in opposite direction, will be longer than the succeeding time interval between the smaller and larger pulses. However, the periodicity of the oppositely directed pulses within the round trip time of the optical cavity will be the same. The asymmetrically timed mode-locked pulses do not cross at the plane mirrors of the optical cavity. They will not generate an interference pattern.

In conclusion, the periodic modulation in time of the optical waveform of the laser array can possibly be explained by mode-locking of the intensity pulsations of the lasers in the array which form a ring laser. By adjusting the distances between the lenses and the plane mirrors in the optical cavity - spontaneous mode - locking of the longitudinal modes can be

obtained. The oppositely directed waves in the ring laser will take up the shape of mode-locked pulses. The periodicity of the oppositely directed mode-locked pulses will be the same. but they are not timed symmetrically because of slight asymmetries in the lasers and the optical cavity. Because of the asymmetry timing, the oppositely directed pulses do not form an interference pattern at the output mirror of the optical cavity. Because of the short coherence time of the intensity fluctuation of the Ga As laser of approximately 2×10^{-12}s, the asymmetry in timing of the oppositely directed mode-locked pulses need not be more than 2×10^{-12} sec., to prevent the formation of an interference pattern. The periodicity of the mode-locked pulses will energize the spiking resonance of approximately 200 MHz. The asymmetry in timing will not prevent the synchronization of the spiking resonance in both Ga As lasers forming the ring laser, because the timing asymmetry is much smaller than the period of the spiking resonance. Mode-locking of the intensity fluctuations in the ring laser should result in increased efficiency of energy extraction from the inverted electron population by the optical field.

6. Design changes of laser device to incorporate spatial filter for laser array

To operate a laser array in the laser device, rather than a single laser, the aperture limiting slit in the building block A51-8007* is omitted. The totally reflecting mirror is replaced by a golden strip of the 140 microns width and 0.97 reflectivity.

In the laser device operating with a single Ga As laser, the aperture limiting slit is placed in front of the totally reflecting mirror. Because of mechanical considerations the distance between aperture and plane mirror is approximately 0.1 cm, that is a tenth of the focal length of the internal lenses. An aperture at this distance of i.e. 130 microns width (which selects the lowest order transverse mode of each laser in the array in the free running mode) cuts off the optical field of the off-center lasers in the array, at a field strength which is e^{-1} that at the center of the mode. In fact, we have observed experimentally that the losses introduced by the aperture increases the threshold currents and the time delay of the off-center lasers in the array.

The assembly of the holder with the spatial filter is shown in Fig. 6.1. The spatial filter for the free-running mode is implemented by the single gold strip of 140 microns width on a disc of fused silica. The disc, outside the gold strip, is covered with black paint to reduce the photon life time of higher order modes. The disc is held in part 531-4008 with a thin plate and four small screws (not shown in the figure). Part 531-4008 is held in part 531-4007 by four screws. To center the strip in reference to part 531-4007, three small screws

* The part numbers refer to the part numbers in the detail drawings of the laser device, built for NASA-MSFC under contract NAS 8-11974 and NAS 8-30543. The assembly drawing is shown in Fig. 2.2.

Fig. 6.1 Holder for spatial filter

through the sidewall in part 531-4007 were added. After the strip is centered, the screws 531-4006 and 0-80 x .188 were tightened.

The holder with the spatial filter is mounted in the building block part A51-8007, the distance between the spatial filter and the lens in building block A51-8007 is established by inserting a small nylong ring of 0.6245 in. diameter in the space between part 531-4007 and the corresponding opening in the building block A51-8007. The thickness of the nylon ring had been established experiementially for each laser array. The holder with the spatial filter is held in building block A51-8007 by the plate 531-4009.

Theoretically, the spatial filter should be placed at the focal plane of the internal lens. Should the spatial filter accidentially be placed a certain distance away from the focal plane, then the waves from the off-center lasers of the array, will not be reflected correctly by the spatial filter. If, for example, the spatial filter is too close to the lens by 0.1 cm, then the reflected waves will effectively come from points on the focal plane which are 46 microns off the optical axis. The reflected waves, on their return trip, will not traverse the symmetrical off-center laser parallel to the optical axis, but tilted by an angle of 0.5×10^{-2} radian. However, the Ga As laser in the array do not operate as a linear amplifiers but rather like amplifying lenses. For this reason the distance between the spatial filter and the internal lens for highest optical power, is not exactly equal to the focal length of the internal lens.

7. Increase in Length of Optical Pulses of Spatial Coherence, at Room Temperature

To meet the requirement of the NASA contract to generate, at room temperature, optical pulses of 400 ns duration, in the spatially coherent mode, IBM had proposed to use LOC heterostructure lasers. This material had been developed at IBM-FSD, Owego, in the previous years and could be grown with reproducable characteristics. However, after IBM's proposal had been submitted to NASA-MSFC, the effort in Owego was discontinued.

To find another source for obtaining heterostructure material for the NASA contract, the Injection Laser Technology Group of IBM's Research Division was contacted. This group has developed for several years double heterostructure laser material for CW operation and had agreed to grow material for pulsed operation to the design of the project manager in IBM Gaithersburg.

As a second source, single heterostructure slivers and LOC heterostructure slivers werepurchased from "Laser Diode Laboratories; Inc" in Metuchen, New Jersey.

Finally, homostructure lasers, and laser arrays, which had been diffused at IBM-FSD Gaithersburg, prior to the NASA contract, were tested to determine whether optical pulses of several hundred nano seconds can be generated.

The length of optical pulses in a semiconductor laser is limited by the temperature rise in the p-n junction introduced by the fraction of the pumping power which is not emitted as

light. Heat is produced in the junction plane at a rate which is proportional to the product of the injection current and the bandgap voltage. Heat is also produced in the entire semiconductor by resistive heating by the injection current passing through the semiconductor material.

The temperature of the p-n junction begins to rise as the injection current is turned on, proportional to the square root of time. The thermal energy starts penetrating into the adjacent p- and n- regions of the laser, but very little penetrates further than the distance x which increases with the square root of time. The penetration depth x in the Ga As laser approaches 7 microns after 400 ns. This distance is small especially in comparison to the thickness of the p- and n- region of the homostructure Ga As lasers which had been diffused in our laboratories, which is 20 microns and 50 microns, respectively.

Because of the small penetration depth, the heat sinks of the laser cannot improve the transfer of heat from the p-n junction to the surrounding material. The temperature rise in the p-n junction limits the duration of the optical pulses since the temperature rise in the junction plane adversely affects the electronic processes in the semiconductor. For longer optical pulses at room temperature, heterostructure semiconductor lasers have to be used where lower threshold current densities and higher differential quantum efficiencies are achieved primarily by confinement of the injected electrons by one or two steps in energy.

The effort at IBM Research on growing heterostructure laser material for pulsed operation never produced satisfactory results. The design parameters for the first wafer to be grown at IBM Research, were specified by the project manager in Gaithersburg. They were derived as follows:

The characteristics for the heterostructure material to meet the requirements of the NASA contract are:

High external quantum efficiency

Threshold current density approximately 10.000 A/cm^2

Catastrophic damage at more than 40 W/mm

Spacing between active region and contact area approximately 6 microns.

The high external quantum efficiency is required because the optical peak pulse power of the spatially coherent Ga As laser is limited by saturation. The saturated gain coefficienc g is related to the unsaturated gain coefficient g_o and the steady state radiation intensities w_+ and w_-, travelling back and forth in axial direction in the laser according to the relation

$$g(z) = g_o \left(1 + \frac{w_+}{w_c} + \frac{w_-}{w_c}\right)^{-1},$$

where w_o is a saturation parameter.

In the spatially coherent Ga As laser the intensities of the waves travelling back and forth is larger at the center of the Gaussian mode than at its wings, resulting in a non-uniform transverse distribution of the saturated gain. The non-uniform gain distribution limits the optical power in the TEM_{oo}-mode.

To accomplish that saturation occurs at higher power, a material with a large unsaturated gain coefficient is required. The unsaturated gain coefficient can be approximated by

$$g_o = \frac{A}{d} \Gamma J^m$$

where A is a proportionality factor, d is the thickness of the active region, Γ is the confinement factor (confinement of the optical field to the active region), J is the injection current and $m \approx 2$. Since the current increases with d, the gain g_o is largely independent of the thickness of the active region. For large unsaturated gain the confinement factor Γ should be close to one.

To accomplish the larger gain we have deviated from the original program of growing an LOC (Large Optical Cavity) structure, primarily because the confinement factor in the LOC structure is always smaller than one. Instead the first structure to be grown at IBM-Research for the NASA contract will be a DHS (Double Heterostructure) with an active region 1.4 microns.

The threshold current density of approximately 10.000 A/cm^2 seems to be an optimum value to obtain 2-3 watts peak pulse power from a single laser diode of approximately 300 microns x 380 microns, at a pump rate J/J_{th} of approximately 2, using pulses of 400 ns time duration. (The pump rate is limited by the anti-reflection coated mirror faces of the laser diodes. Because of the finite reflectivity of these coatings, an increase in pump rate could result in generation of internal modes.)

In order not to damage the mirror faces of the Ga As laser diodes, material must be used where catastrophic degradation occurs at more than $40 \frac{W}{mm}$. This requires that the active region be wider than 1 micron.

The spacing between active region and contact area of approximately 6 microns represents a compromise between the requirement to set up a self-reproducing field in the laser with the external optical cavity, and a good heat transfer from the active region to the heat sink.

To investigate the properties of DHS laser with wide active region, lasers made from DHS material (257), grown by the Injection Laser Technology group of IBM's Research Division (Prior to the NASA contract) have been tested. The active region of this material is 1.1 microns wide.

The tests were performed on lasers radiating in a multitude of transverse modes. No tests could be performed in the laser device with the external optical cavity and the transverse mode control. Because in the material 257 the active region is spaced only 3.6 microns from the contact, a self-reproducing field could not be set up.

A tentative evaluation of the material 257 indicates that its optical properties are close to those required for the contract with the exception of the limit of catastrophic degradation which was approximately $20\frac{W}{mm}$.

Extrapolating from the measured parameters of the material 257, the following double heterostructure material will be grown at IBM-Research for the NASA contract.

		t	Al content
p^+	Ga As	15 microns	0
p	Ga AlAs	$<$ 1 micron	x%

p	Ga As	1.4 microns	0
n	Ga AlAs	$<$ 1 micron	y%
n	Ga As	$<$ 70 microns	0

The larger thickness of the active region in comparison to the material 257, seems to be required for the catastrophic degradation to occur at higher optical power. The larger thickness of the p^+ Ga As region seems necessary to assure the proper feedback in the laser device with the external optical cavity. The thickness of the p^+ region of 15 microns has an adverse effect on the heat transfer from the active region to the heat sink. However, the new material should serve primarily as a test model to establish the optical properties of the laser material. An improvement in heat transfer will be considered later in the program.

The doping of the epitaxy layers and their Al content should be made similar to those in the material 257. However, we suggest to increase the doping in the p^+ Ga As layer if possible, primarily to reduce electrical and thermal resistances in this layer.

The material growth was initiated June 6, 1974.

The first wafer which had been grown at IBM Research for the NASA contract did not have good properties. IBM Research indicated that during the growth of the wafer impurities had accidentally entered the growth apparatus.

The second wafer (OT-2) had better properties in multi-made operation but the metallization was non-uniform and the wafer thickness varied from 60 microns to 115 microns. Because of the thickness variations the material became cracked in their holders while being anti-reflection coated.

Three more wafers of the same design were grown at IBM Research. None of the wafers yielded lasers with satisfactory properties. Parallel to the effort of growing the double heterostructure wafers OT-3 and 5, for the NASA contract, we proceeded with the evaluation of LOC heterostructures, as an alternate design to also be grown at IBM Research.

A study of the literature on pulsed room temperature heterostructure Ga As lasers indicates that the PpnN structure developed by the Bell Telephone Laboratories for use in fiber communication systems, will lend itself well for use in the optical cavity of the single transverse mode device. The design parameters of this structure were outlined in the papers in the Journal of Applied Physics, vol. 44, p. 1276, 1973 and vol. 45, p. 2168, 1974. These design parameters are summarized in the following. The various layers of the large cavity Ga As PpnN laser were grown by liquid phase epitaxy method. The total waveguide thickness is approximately 2 microns. The waveguide is subdivided into the active p-region of1.1 microns, doped with Ge to a level of 4×10^{17} cm^{-3} and the n-region doped with 3×10^{18} cm^{-3} Te, and also with addition of 3% AlAs. The small addition of Al is meant to improve the carrier confinement. The ternary p-$Ga_{0.6}$ $Al_{0.4}$ As region is followed by a heavily doped p-type Ga As layer. The ternary n-region has the same Al content as the ternary p-region. The thickness between active region and metal contact is 3-5 microns. (It is important that in the PpnN structure to be grown for the NASA contract, this thickness be increased to 15 microns to facilitate to optical feed-back.)

In September 1974, the growth apparatus at IBM Research became inoperative until April 1975. After this delay an

attempt was made to grow the LOC structure for the NASA contract which had been specified by the project manager. However, the layer thicknesses deviated considerably from those which had been specified. End of April the effort at IBM Research had to be discontinued because of lack of funds.

In conclusion, though an attempt had been made to develop heterostructure material for pulsed operation at IBM Research the effort was too small. The development of a new structure requires a larger effort than could be supported by the NASA contract.

The single heterostructure material purchased from "Laser Diode Laboratories" had been tested in multi-mode operation and was also AR coated and tested in the spatially coherent mode. In the spatially coherent mode the lasers, made from the SHS material, have shown H-pulsing. H-pulsing refers to abnormal behavior where the optical pulses do not coincide with the injection current pulses but only short optical pulses occur at the beginning and end of the current pulses. It seems that the "transition temperature" between normal and abnormal behavior of the SHS laser material from "Laser Diode Laboratories" is only slightly above room temperature. When operated in the spatially coherent mode the losses introduced by the spherical aberrations of the lenses in the external cavity, seem to reduce the transition temperature to room temperature and H-pulsing occurs at room temperature already. However, the temperature range of the abnormal behavior of SHS lasers is very narrow, and it could be possible to suppress the H-pulsing by slightly reducing the temperature of the SHS lasers.

The LOC heterostructure material purchased from "Laser Diode Laboratories" was never sufficiently uniform to be tested in the spatially coherent mode.

The tests on the heterostructure material purchased from "Laser Diode Laboratories" was discontinued because the characteristics of the lasers were not adequate. Also, the array geometry, made at "Laser Diode Laboratories" was not suitable for the spatially coherent mode because of the wide spacings between the lasers in the arrays.

Finally, homostructure lasers and laser arrays were tested to determine whether optical pulses, in the spatially coherent mode, of several hundred nano-seconds can be generated. The lasers had been diffused at IBM-FSD Gaithersburg and the junction width of each laser was 190 microns.

Experiments were first performed with a single homostructure laser. We have observed that for current pulses up to 300 ns, the optical peak power in the single transverse mode was fairly constant at 1.6 watts for close to 250 ns, as shown in Fig. 7-1. We also have observed that the optical pulse power in the TEM_{oo} mode only remained constant over close to 250 ns, when, in addition to the transverse mode control at the totally reflecting mirror, a second, slightly wider, aperture at the output mirror was used.

Then, two laser array in spatially coherent, free running mode, was tested with pulses of approximately 250 ns duration. The lenses in the external optical cavity were doublets, corrected for spherical aberrations. The spatial filter was a gold strip of 130 microns width and a shutter of 615 microns

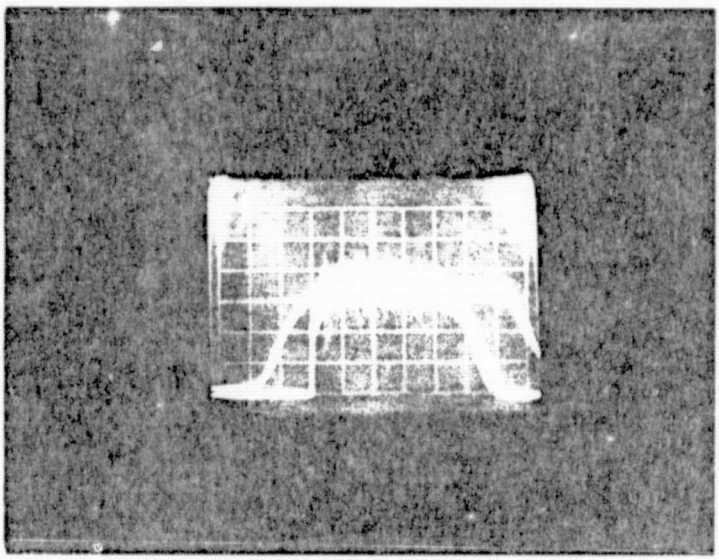

Lower vertical trace: 0.4 W/div

Upper vertical trace: 20 A/div

Horizontal trace: 50 ns/div

Fig. 7-1 Injection current and optical waveform of single laser in lowest order transverse mode. Aperture at totally reflecting mirror: 130 microns, at output mirror: 190 microns

width was placed in front of totally reflecting mirror. The length of the injection current pulses was limited by the transformer and driver. A transformer was used which had been designed for operation with a single laser. (The modified pulse transformer with the larger core area and increase in turns of the primary winding, was not available.) The driver was a transistor driver. The driver which had been designed and assembled to generate pulses of 60A and 400 ns never became operational because of the malfunctioning of the Watkins-Johnson "Electron Bombarded Semi-conductor".

We have observed that the optical peak pulse power in the spatially coherent mode remained fairly constant at 4 watts for close to 200 ns, as shown in Fig. 7-2.

Finally, a three laser array in the spatially coherent, free running mode, was tested in the engineering model of the laser device, with Gaussian pulses of approximately 350 ns half-width. The laser array was operated in the modified pulse transformer with doubled core area and the increase in turns of the primary winding.

The spatial filter was a gold strip of 140 microns width and a shutter of 1000 microns width was placed in front of the output mirror. At the high current level, the pulses generated by the transistor driver were badly distorted.

The optical peak power of the three laser array at the leading edge of the injection current pulse, was close to 5 watts and decreases to 3.5 watts after 200 ns, as shown in Fig 7-3. The droop can partly be introduced by the lower frequency limit of the modified pulse transformer of 10^5 Hz. We have computed that this cut-off frequency results in a

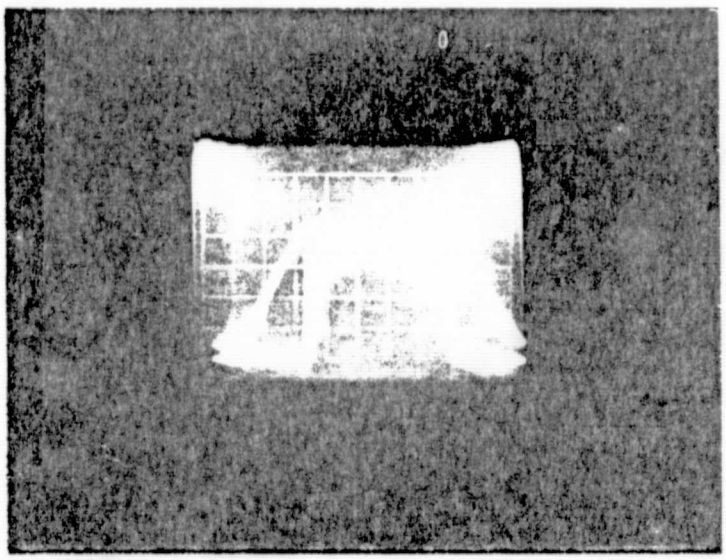

Lower vertical trace: 1 W/div

Upper vertical trace: 30 A/div

Horizontal trace: 50 ns/div

Fig. 7-2 Injection current and optical waveform of two laser array in spatially coherent, free running mode. Spatial filter: 130 microns, aperture at output mirror: 615 microns

Lenses corrected for spherical aberration

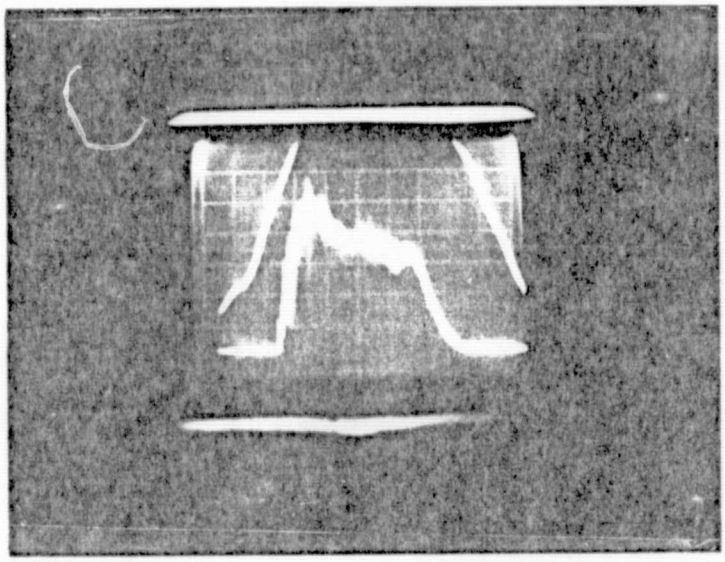

Vertical trace: 1 W/div

Horizontal trace: 50 ns/div

Fig. 7-3 Optical waveform of three laser array in laser device, radiating in the spatially coherent, free running mode. Spatial filter: 140 microns, aperture at output mirror: 1000 microns

decrease of the secondary current of 220 Amp. after 400 ns by 26 per cent. However, the distorted pulses of the transistor driver might introduce a larger droop and also generate excessive heat in the p-n junctions of the array.

8. Modification of pulse transformer for higher energy injection current pulses

The use of an array of homostructure Ga As lasers in the laser device rather than of a single laser, and the required increase in pulse length, made modifications of pulse transformer necessary. The modifications are limited by the requirement that major changes in the design of the laser device be avoided. Within this limitation, the changes which could be made are an increase in core area and an increase in the number of turns of the primary winding.

The design principle of the pulse transformer is shown in Fig. 8.1 which gives the pulse transformer before its modification for higher energy injection current pulses. It is a step-down transformer where the coil of the primary winding (which has the form of a toroid) is wound on a toroidal core. The secondary winding consists of one turn only. A low-impendance transmission line which is terminated by the Ga As lasers is coupled to the secondary winding.

In the modified transformer the toroidal core (C) is a stack of four toroid cores of the part number 266T125 (made by "Ferrocube" North American Philips Company). The core material is of the type 3E2A. The effective cross-sectional area of the core is 0.3 cm^2, its mean magnetic path length is 2.16 cm and the relative permeability is $\mu_e = 1800$. The primary winding has six turns; it is made of an isolated copper strip of 2.5 mm width, and 0.1 mm height, which is tightly wound on the core, covering most of the core material.

The secondary winding of one turn has circular symmetry in reference to the core center; it is formed by the housing

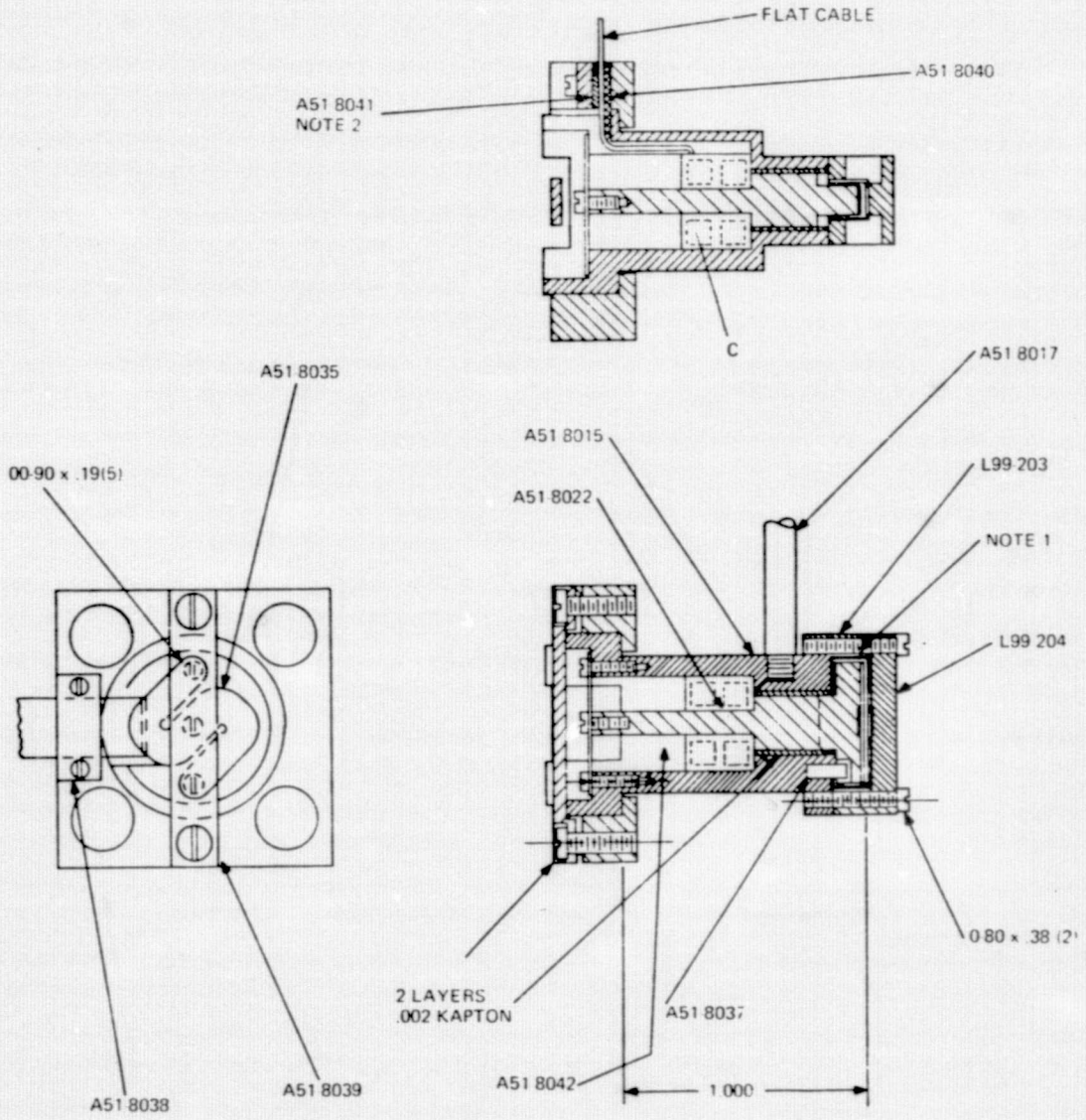

Figure 8.1 Transformer Assembly

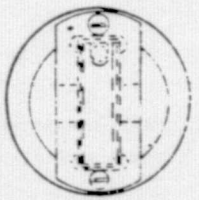

A51-8015, the rod A51-8022, and the block A51-8042. To add two toroid cores the height of part A51-8042 was reduced from 0.36 in. to 0.1 in. The secondary winding of one turn houses the toroidal core with the primary winding and tightly encloses it. (The tight packing is required to minimize the leakage inductance of the transformer).

The low-impedance coaxial transmission lies between the housing A51-8015 and the rod A51-8022, which is terminated by the laser array, is coupled to this secondary winding of the pulse transformer. Because of the continuity of the conduction current in the one turn secondary winding, and the displacement current in the coaxial transmission line, efficient coupling is achieved. In fact, the conduction current vector induced in the upper and lower part of the one-turn winding by the magnetic field in the core, is radial. The electrical field vector in the coupled coaxial transmission line is also radial.

The characteristic impedance of the dielectrically loaded coaxial transmission line $Z_o = \frac{1}{\kappa_e} \ln \frac{r_a}{r_i} = 1.4$ ohm for $r_a = 0.125$ in., $r_i = 0.12$ in. and $\kappa_e \approx 3$; the length of the transmission line is 0.43 in. Because of the low characteristic impedance of the coaxial transmission line and its short length, the impedance of the Ga As diode, transformed to the secondary winding of the pulse transformer, is primarily resistive over nearly the entire frequency band of the pulse transformer. Only at the upper frequency limit does the inductive component of the transformed diode impedance begin to be effective; (at 25 MHz the transformed diode impedance is $Z = 20 \times 10^{-3} + j\ 14 \times 10^{-3}$ ohm). Thus, only at the upper

frequency limit does the reactive power approach the resistive power which is transferred to the Ga As diode, resulting in a slight distortion of the pulse shape.

The configuration of the pulse transformer makes it possible to place the Ga As laser arry along the optical axis of the external resonator and the toroidal core outside the cavity. In fact, the length of the optical cavity can be kept small to minimize misalignment errors which are proportional to the resonator length and need not accommodate the toroidal core whose large diameter is required by the high injection current. The physical separation between laser diode and core has the added advantage that heat generated in the toroidal core by Eddy currents is not directly transferred to the Ga As diode.

Tests on the transformation ratio of the new transformer were performed using a transistor driver with 1 ohm output impedance. The driver generates pulses of Gaussian shape with a half-width of approximately 150 ns. The tests were performed by comparing the transformation ratio of the modified transformer with that of the previous transformer, which had been measured to be 4:1. To do so, different Ga As lasers and laser arrays were mounted alternatively in the two transformers. Then, the current into the primary winding of the transformers was monitored which yielded the same optical output power. Using a single Ga As laser of 12 mil junction width in the transformers, the new transformer requires 0.67 of the primary current of the previous transformer. Using a two laser array of 12 mil junction width, the new transformer requires 0.5 of the primary current of the previous transformer. Also, the half-width of the primary current pulses of the new transformer is approximately 140 ns, while the half-width using the previous transformer is approximately 90 ns.

Tests of the frequency characteristic of the pulse transformer would require a pulse generator with 1 ohm internal impedance which generates pulses of at least 40A and 400 ns duration. Though we have designed and assembled this type of pulse generator, the malfunctioning of the Watkins- Johnson "Electron Bombarded Semi-conductor" has prevented us from using it.

We conclude from the tests which we could perform, that the transformation ratio of the modified transformer is 6:1. The change in the current relation from 0.67 to 0.5 at approximately 100A in the secondary winding, indicates, that, at this current level, the previous transformer starts saturating while no saturation seems to occur in the modified transformer.

The wider band-width of the modified transformer becomes apparent from the wider half-width of its primary current. The waveform of the primary current is that of the driver which becomes distorted by terminating it with the complex impedance of the pulse transformer. The wider band-width of the modified pulse transformer means, in effect, that its impedance is real over a wider range of frequencies, thus introducing less distortions on the waveform of the driver.

In conclusion, the modified transformer with the larger core area and the increase in turns of the primary winding, has a transformation ratio of 6:1, saturates at higher injection currents and has a wider band-width than the previous transformer.

9. Increased Stability

To increase the stability of the laser device, developed under contract NAS 8-11974, IBM had proposed a) to improve the control of the position of the laser array in the optical cavity and b) also to facilitate the transition from mechanical to electro-mechanical alignment control.

a.) The construction of the laser device is such that the Ga As laser array is housed in the pulse transformer, Fig. 8.1. The laser array had been held between the parts L99-204 and A51-8022, by the spring A51-8035. To improve the mechanical stability of the laser device, one heat sink of the semi-conductor laser array, is soldered to the part L99-204, which is an integral part of the transformer housing. For this connection low temperature solder is being used which melts at lower temperature than the indium which connects the semi-conductor laser array to the heat sinks.

Soldering the heat sink to the large copper part L99-204 also improves the transfer of the heat, generated in the p-n junctions of the laser array, to the transformer housing. The heat sink which is soldered to the large copper part, is connected to the p-region of the semi-conductor array, which is always narrower than the n-region. The heat is now transferred through a path of good heat conductivity from the p-n junctions of the array and through the narrow p-region, to the large transformer housing.

b.) For the alignment of the laser device a transition is required from mechanical alignment (in direction perpendicular to the junctions of the laser array) by means of parts A51-8019 and 8034, to an electro-mechanical alignment by means of two

piezo-electric transducers, parts A51-104. During this transition, mechanical stresses can accidentally be exerted which can move the lenses in the holders, parts A51-8009, out of alignment. The stresses result from an accumulation of small deviations, which take place when the transducer housings, parts A51-8030, are clamped down in part A51-8028. In the model of the laser device which operates with the laser array, misalignments occur which are too large to be corrected by the electro-mechanical alignment control.

To facilitate the transition from mechanical to electro-mechanical alignment control during the alignment procedure of the laser device, a coupling device was inserted between the holders, part A51-8009, of the external optical cavity and the piezo-electric transducers, part A51-104. This type of mechanical improvement was easier to incorporate than an improvement using piezo-electric transducers with larger deviation.

To insert the coupling device, the stiff mechanical coupling rod, part A51-8029, between the piezo-electric transducer, part A51-104 and the holder for the lens - mirror housing, part A51-8009, was cut through and both remaining ends were threaded, as shown in Fig. 9.1. The divided coupling rod was bridged by part 531-4001, shown in Fig. 9.2. A rotation of the part 531-4001 can compensate for misalignments which can result from mechanical stress during the transition from mechanical to electro-mechanical alignment control. After the transition is completed and any misalignment is compensated, using the coupling device, the electro-mechanical alignment correction by means of the piezo-electric transducers can operate over its full range.

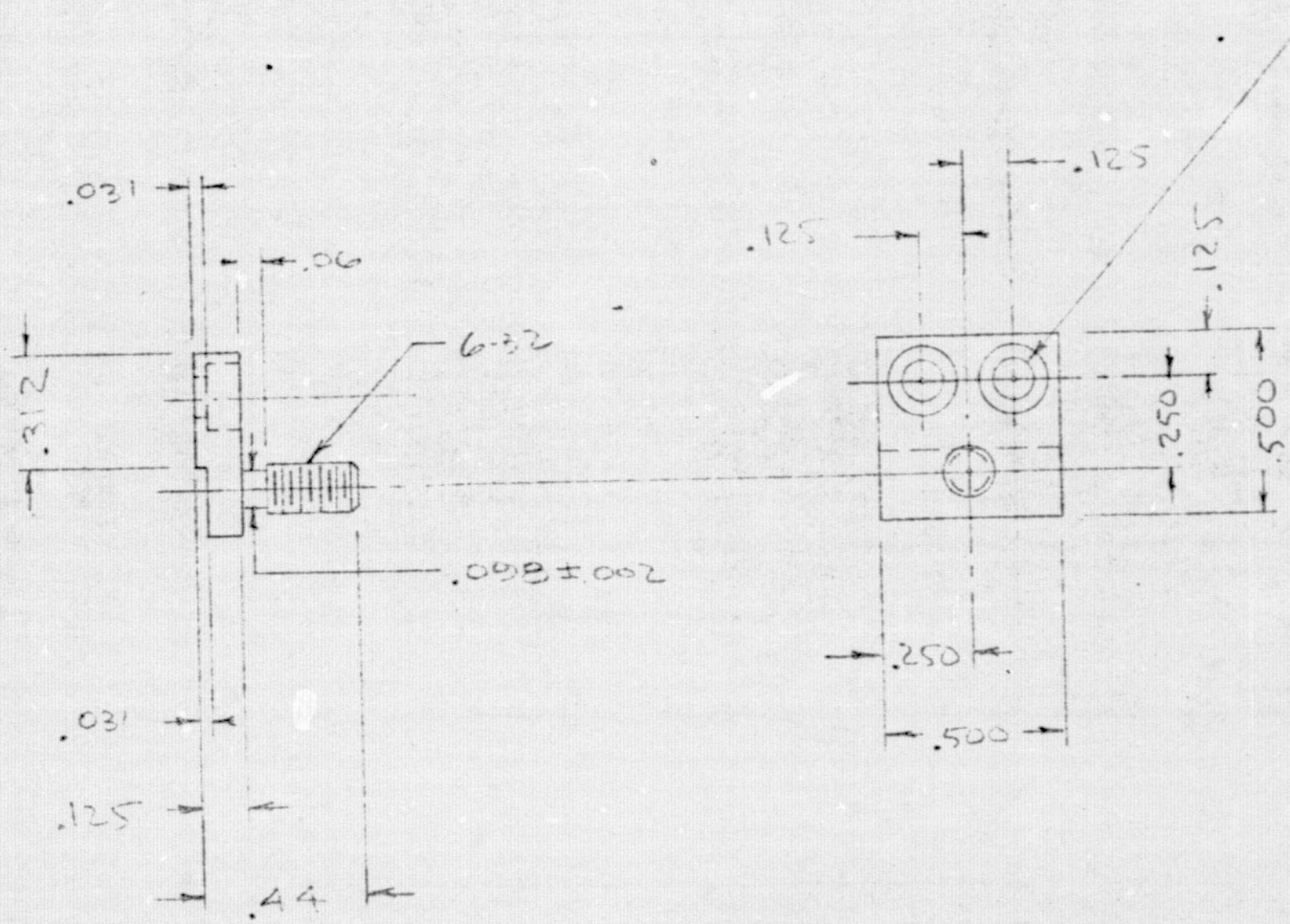

TOL: 2 PL ±.02
3 PL ±.005
MATL: STAINLESS STEEL
SCALE: 2/1
QTY: 2

POST, TRANSDUCER
531-4002

Fig.9.1 Transducer post

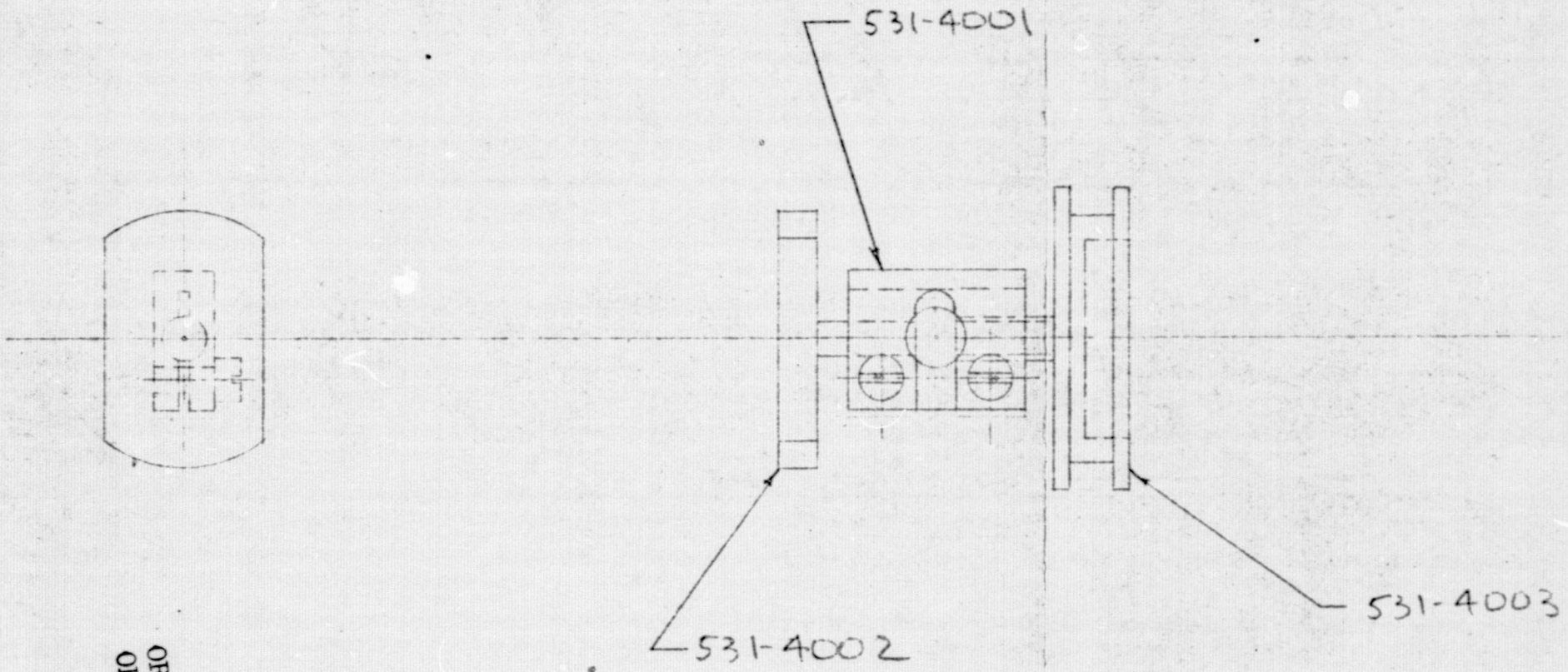

Fig. 9.2 Transducer coupling assembly

It should be mentioned that the insertion of the coupling device presents a deviation from the design principle of the laser device, where all parts are locked in position. The coupling device is not required, should the piezo-electric transducers be made to closer mechanical tolerances.

A summary on an investigation on piezo-electric transducers for the laser device is given in the following section.

10. Piezo-electric Transducers

We have investigated whether the piezo-electric transducers in the laser device could be replaced by structures which can yield larger expansion or contraction than presently obtainable.

In the original design of the laser device each transducer was a stack of thin piezo-electric plates from Vernitron Corp., with a cross-section of 0.5 inches x 0.5 inches and an overall length of 2 inches. The plates of 0.030 in. thickness were connected electrically in parallel. They were rated for a maximum thickness variation of $\pm$ 15 microns for a voltage swing of $\pm$ 500 volts. The piezo-electrical crystal stack could theoretically exert the required force of 1 pound to move the optical components by 15 microns.

However, the stacks could not be used. Though the plates were rigid, the adhesive which holds the plates together was too brittle and broke when the stacks were mounted in the laser device.

Each stack was replaced by a piezo-electric cylinder. The transducers which are presently in the two laser devices are ceramic cylinders of the type G1512, made by Gulton Industries, Inc., in California. Each cylinder has 1 in. diameter (D), 2 in. length (L) and 0.062 in. wall thickness (d). The cylinders are operated in the transverse mode, where the length variation $\pm \Delta L$ is

$$\pm \Delta L = L \frac{\pm V}{d} d_{31}$$

V is the applied voltage and $d_{31} = 232 \times 10^{-12}$ m/volt. For a voltage variation from + 1000 volt to - 1000 volt, the length variation should be 15 microns. (This length variation was never obtained.)

The cylinders are very rigid, the force which each crystal can exert is

$$F = \frac{V\pi D}{g_{31}}$$

where $g_{31} = 9.3 \times 10^{-3}$ volt-m newton. For a voltage of 1000 volts the force is 2000 pounds, it by far exceeds the required force to move the optical components.

We have contracted three different companies who are known for their capabilities in manufacturing piezo-electric transducers. They are:

a) Gulton Industries, Inc., Fullerton, California. They manufacture ceramic cylinders and would, under special order, build stacks of ceramic plates. The type of cylinder which presently is used in the laser devices is not available any longer. Instead, we would have to use a cylinder of the same dimensions except with 0.125 in. wall thickness. This type of cylinder requires twice the voltage of obtain the same length variations as the cylinders with 0.062 in. wall thickness.

For the material G1512 the positive voltage to the piezo-electric cylinder is limited to 70 volt/mil or to 8750 volts for 0.125 in. wall thickness. The negative voltage is limited by depoling to approximately $\frac{Ec}{2}$, where $\frac{Ec}{2} = \frac{6\ kV}{cm}$, or to 1900 volts for 0.125 in. wall thickness. Using the material G1278 the coefficient d_{31} is 270×10^{-12} m/volts, yielding an increase in length variation by a factor 1.16. The limit to the positive voltage is the same as for the material G1512, the limit to the negative voltage is 1100 volts. The ceramic cylinders can operate on compression and tension. Both types of cylinders should yield length

variations of 40 microns when used over the entire voltage range. The price is $15.75, the minimum purchase is $150.00.

b) Burleigh Instruments, Inc., Rochester, N. Y. They manufacture an assembly, consisting of a stack of three ceramic cylinders in a holding structure, type PZ400. The overall length is 1.83 in., the outer diameter is 0.65 in. and the wall thickness of the ceramic cylinders is 0.018 to 0.020 in. The three stacked cylinders produce a length variation, from 0 to 15 microns for a voltage swing from 0 to 1000 volts. The piezo-electric transducer assembly PZ40 can only operate on compression. The force it can exert is 35-40 pounds. The price is $165.0.

Burleigh also would manufacture stacks of ceramic plates on a special order, with 1.4 in. length, 0.5 in. outer diameter, made of plates with 0.050 in. thickness. The length variation would be 20 to 25 microns for a voltage variation from 0 to 1000 volts, the force the stack could exert would be 20 pounds, the price $300.00 and the delivery 3-4 weeks.

c) Physics International Co., San Leandro, California, manufactures stacks of piezo-electric plates. The length of a typical stack is 2 in., the outer diameter is 0.75 in., and the thickness of the plates is 0.050 inches. The free displacement is 74 microns for a voltage swing from 0 to 1500 volts. The stack can exert a force in excess of 1000 pounds. The transducer only works on compression. The price was quoted for a stack of 3 in. length and 0.5 in. diameter as approximately $350.00, delivery is very short term.

In summary, the simplest approach would be to use the ceramic cylinders which are presently in the laser devices or to replace them with new ceramic cylinders from Gulton Industries. To increase the length variations it would be required to make the positive voltages larger than 1000 volts. This approach is only possible if voltages higher than 1000 volts can be used in spacecrafts.

Should the voltages be limited, the stacks of ceramic plates should be used which yield larger length variations for a voltage swing from 0 to 1000 volts. The larger length variations, however, can only be obtained in compression.

The two stacks of piezo-electric discs of the type PZWT 100 were ordered from "Physics International Company" and were received in April 1975. The outer diameter of the discs is 0.5 in., the length is 2.04 in. and the disc thickness is 0.03 in. Each transducer should yield a change in length of 48 microns for a voltage swing from 0 to 1000 volts. The price was $400.00 per stack.

With the transducers, we received instruction from "Physics International Company" that each stack must be held in place by a suitable compression load. The preload should never fall below about 50 pounds.

Though we had been aware that a compression load was required, we had not been told previously, the magnitude of the load. According to information from "Physics Internation Company," the preload is required for linearity of the mechanical deviation with voltage, but also to prevent the stacks from being damaged.

The contract management at NASA-MSFC in Huntsville and at IBM-FSD in Gaithersburg has agreed not to incorporate the stacks of piezo-electric discs (at the present time) in the laser device for the following reasons: The mechanical stability of the device has been improved under the present contract by soldering the lasers to the transformer cap and also by mechanical changes of the transducer coupling. Stacks of piezo-electric discs are much less stable than the solid piezo-electric cylinders presently used in the laser device. Also, the complexity required by a compression load of 50 pounds might introduce new problems.

11. Alignment Procedure

The alignment of the engineering model of the spatially coherent laser array with the external optical cavity, is performed in five steps, they are:

1. Alignment of external optical cavity with the use of two collinear He-Ne lasers.

2. Alignment of Ga As laser array inside the resonator, perpendicular to the optical axis, with the right He-Ne laser.

3. Alignment of Ga As laser array inside the resonator by observing the image formation using the incoherent light of the Light Emitting Diode Mode of the laser array.

4. Alignment of the spatial filter and the shutter at the output mirror, using the two He-Ne lasers.

5. Transition from mechanical resonator alignment to electro-mechanical alignment control.

1.1 To align the external optical cavity, first the building blocks A51-8007 and 8008, must be assembled. (The part numbers refer to the part numbers in the detail drawings of the laser device, built for NASA-MSFC under contract NAS 8-11974 and NAS 8-30543. The assembly drawing is shown in Fig 2.2.In this figure the building block A51-8005 and 8006 for the corrected lenses are shown, rather than the building blocks A51-8007 and 8008). In the building blocks A51-8007 and 8008 the single plane-concave lens is mounted with its curved surface towards the plane mirror, it is rigidly held in position by two screws.

In the building block A51-8007, for the alignment steps 1, 2 and 3, the spatial filter must be repleced by the plane, totally reflecting mirror (used for the earlier design) which is held in the building block A51-8007 by the plate A51-8031. The plane mirrors in the building blocks A51-8007 and 8008 are marked to assure correct orientation of the surfaces with the reflectivities R=0.998 and R=0.2. The plane mirrors must be mounted with the opening of the sign " " on the rims of the mirrors, pointing towards the lenses of the optical cavity. A nylong ring of 18 mil thickness is placed between the totally reflecting mirror and the building block A51-8007 to facilitate alignment corrections of the mirror, perpendicular to the optical axis of the lens.

The building block A51-8008 is assembled similar to the assembly of building block A51-8007. The plane mirror in building block A51-8008 has a reflectivity of 0.2. In the building block A51-8008 more than one nylon ring is placed between the mirror and the building block. The thickness of these rings was determined experimentally for the different laser arrays to be used in the laser device.

The distance between the two building blocks along the optical axis is controlled by rings between the building blocks A51-8007 and 8008, and the brackets A51-8009. The thickness of the rings is specified for the different laser arrays to be used in the laser device.

1.2 Then the building block A51-8007 is locked in position in the right bracket A51-8009. The lens in building block A51-8007 is aligned to be perpendicular to the two He-Ne laser beams. For the lens alignment the entire laser device is being

moved. The lens is perpendicular when the interference rings, formed by the superposition of the waves reflected from the curved and plane surfaces of the lens, are symmetrical in respect to the right He-Ne laser beam, and the reflection of the left He-Ne beam, from the plane lens surface, is parallel to the laser beam.

Next, the lens center is adjusted to coincide with the center of the right He-Ne laser beam. This is accomplished by observing the symmetry of the magnified right He-Ne laser beam on a close-in target to the left of the laser device. In doing so the He-Ne laser beams become collinear with the optical axis of the Ga As laser device.

The precision alignment of the lens in the building block A51-8007 is important, because later the interference of the spherical waves from the two surfaces of the lens, with the reflection from the cleaved surface of the Ga As laser array, are used to align the cleaved surface of laser array to be perpendicular to the optical axis of the resonator. By aligning the lens, the totally reflecting mirror also becomes aligned perpendicular to the optical axis. (This is ensured by the precision construction of the building block. Small alignment corrections can be accomplished by exerting pressure by means of the three screws in the plate A51-8031). The alignment of the mirror perpendicular to the optical axis is controlled by observing the reflection of the right He-Ne beam. The alignment of the totally reflecting mirror serves as reference to control accidental motions of the laser device during later steps of the alignment procedure.

1.3 The assembled building block A51-8008 is mounted in the left bracket A51-8009. The construction of the laser device is performed with sufficient accuracy to ensure that the center of the second lens coincides with the optical axis, established by the lens in the building block A51-8007. For small corrections in the vertical direction, required by possible dislocations of the optical lens centers in reference to the mechanical lens centers, the building block A51-8008 must be rotated until the He-Ne beam from the right laser, transformed by both lenses, becomes collinear with the He-Ne beam in vertical direction. (This is observed by the symmetry in vertical direction of the transformed laser beam on the left target). Then, the building block A51-8008 is locked in position. To accomplish that the He-Ne beam from the right laser, transformed by both lenses, becomes also collinear with the He-Ne laser in horizontal direction, the building block A51-8008 is moved by means of part A51-8019.

To complete the alignment of the optical cavity, the partially reflecting mirror is aligned to be perpendicular to the left He-Ne laser. To do so, pressure is exerted by means of the three screws in the plate which holds the mirror.

2.1 Then the Ga As laser array must be mounted in the pulse transformer. In the engineering model of the laser device, the pulse transformer which houses the laser array, is an integral part of the device. In the transformer, the laser array is placed between part L99-204 (part A51-8021 in Fig. 1), and part A51-8022. For greater stability, and better heat transfer, the heat sink which is connected to the p- side of the semi-conductor lasers (marked with three crosses) is soldered to part L99-204.

Care must be taken in mounting the laser array, since the height of the Ga As bars, from which the lasers are made, can vary by approximately 20 microns and the thickness of the headers by as much as 150 microns. (These variations obviously could be reduced). To control the pressure on the laser array, the distance between the part L99-204 and A51-8022 can be adjusted for the different arrays by adding thin pieces of copper to part A51-8022.

The pulse transformer is mounted in the block A51-8014. The transformer is held by the clamp A51-8039 and the plate A51-8013. The block A51-8014 is movable along the optical axis of the laser device, as well as in direction along the p-n junctions of the laser array. These two motions are controlled by the bridge A51-8033. The pulse transformer can also be rotated using part A51-8017 which is removable. The bridge which is mounted on the bracket A51-8011 can be removed after the alignment is completed and all parts are locked in position.

2.2 To align the laser array inside the optical cavity, first the mirror faces of the lasers must be aligned to be perpendicular to the optical axis of the cavity. This alignment which is only required along the p-n junctions, is accomplished by rotating the pulse transformer by means of part A51-8017 and by observing the symmetry of the coherent reflection of the He-Ne beam from the mirror face of the laser diode. To align the lasers properly, they are moved along the optical axis by approximately 0.1 cm, where the beam diameter of the He-Ne laser, focused by the lens in the optical cavity, is approximately the same as the diode height. Two sets of interference rings are observed. Small bright rings which result from superposition of the reflections from the mirror

face of the diodes and the plane face of the lens in the optical cavity; and large dark rings which result from the superposition of the reflections from the same surfaces, but also from the diverging wave from the mirror face which is reflected by the mirror and the plane face of the lens in the optical cavity. These additional reflections increase the magnification of an alignment error. For greater precision, therefore, the symmetry of the large dark rings is observed. The pulse transformer in the Ga As laser device is rotated until the small and the large interference rings become symmetical to the He-Ne laser beam in vertical direction, indicating that the mirror faces of the laser array are perpendicular to the optical axis in the direction of the p-n junctions. Then the rotational motion is blocked by locking the pulse transformer in position in the block A51-8014 using the clamp A51-8039. Part A51-8017 is now removed and the pulse transformer is moved closer to the center of the optical cavity by means of part A51-8002.

3.1 Next, the laser array must be placed exactly at the center of the external optical cavity. This alignment process does not require the He-Ne laser but uses the spontaneous emission of laser array. To do so, the primary winding of the pulse transformer is connected to the strip transmission line with 1 ohm characteristic impedance, with the inner lead of the pulse transformer being connected to the positive terminal of the pulse generator. The pulse generator is turned on to produce pulses of 5 Amperes peak value. Then, the totally reflecting mirror is removed and we observe with the image converter, set to infinity, the spontaneous emission from both mirror faces of the lasers, magnified by the lenses in the optical cavity.

3.2 To align the laser array to be exactly symmetrical in reference to the length dimension of the optical cavity, the block A51-8014 which houses the pulse transformer, is moved along the optical axis by means of part A51-8002, until the magnified p-n junctions of both mirror faces look very similar.

3.3 To align the laser array to be exactly symmetrical in reference to the horizontal and vertical dimension of the optical cavity, the images of the p-n junctions, formed in the optical cavity, are aligned with the p-n junctions on the mirror faces. For this alignment, the totally reflecting mirror is again placed in the building block A51-8007 and aligned perpendicular to the optical axis.

First, the image is observed through the partially reflecting mirror. The image of the junction, formed by the lens and mirror in building block A51-8007, is aligned with the image on the mirror face, perpendicular to the junction, by moving the building block by means of the part A51-8034. The image, formed in part A51-8007, is moved through the n region to the p-n junctions by counter-clockwise rotation of the screw controlling part A51-8034.

Then the images are aligned along the junctions by vertically moving the block A51-8014, by means of the screw A51-8001. When these alignments ar accomplished, the movable block A51-8014 is locked in position by tightening the plate A51-8013 to the bracket A51-8011.

Then the totally reflecting mirror is removed and the image is observed through the lens in building block A51-8007. The image formed by the lens and mirror in building block A51-8008 is moved perpendicular to the junctions, through

the n-region to the p-n junctions by counter-clockwise rotation of the screw controlling the part A51-8019. Proper alignment of the optical cavity assures that the images are aligned correctly along the p-n junctions.

The nylon spacer is now removed from part A51-8007.

4.1 The holder with the spatial filter is assembled. The assembly is shown in Figure 6.1. The spatial filter is implemented by a single gold strip of 140 microns width on a disc of fused silica. The disc, outside the gold strip, is covered with black paint to reduce the photon lifetime of higher order modes.

The disc is held in part 531-4008 with a thin plate and four small screws (not shown in the figure). Part 531-4008 is held in part 531-4007 by four screws. To center the strip in reference to part 531-4007, a microscope alignment technique is used. To facilitate the strip alignment, three small screws through the sidewall in part 531-4007 were added. After the strip is centered, the screws 531-4006 and 0-80 x .188 are tightened.

4.2 The holder with the spatial filter is mounted in part A51-8007, the distance between the spatial filter and the lens in building block A51-8007 is established by inserting a small nylon ring of 0.6245 in. diameter in the space between part 531-4007 and the corresponding opening in the building block A51-8007. The thickness of the nylon ring had been established experimentially for each laser array.

4.3 The holder with the spatial filter is held in building block A51-8007 by the plate 531-4009. Before the plate is tightened the holder with the spatial filter which is rotatable in part A51-8007, must be rotated until the gold strip becomes exactly perpendicular to the laser array. For the rotation the two screws 531-4006 are used and the coherent reflection of the right He-Ne laser on the gold strip is observed. The coherent reflection from the gold strip is a diffraction pattern, perpendicular to the narrow dimension of the gold strip.

The correct orientation of the diffraction pattern, set up by the coherent reflection from the gold strip, had been established prior to the final assembly of the laser device. To do so, after alignment 2.2 was completed, the building block A51-8008 was removed and the coherent reflection of the left He-Ne laser beam on the cleaved surface of the Ga As laser array was marked on the left target. Then the pulse transformer with the laser array was also removed and the spatial filter in its holder was mounted in the building block A51-8007 and illuminated by the right He-Ne laser. The spatial filter was rotated until the magnified shadow of the gold strip became parallel to the coherent reflection from the mirror face of the Ga As laser array, which had been observed before. Then the orientation of the coherent reflection from the gold strip was marked on the right target.

To proceed with alignment 4.3 the holder with the spatial filter is rotated until the orientation of the diffraction patterns is parallel to the orientation marked previously.

4.4 To align the spatial filter perpendicular to the optical axis of the cavity, the three screws which hold the plate 531-4009 are adjusted until the main lobe of the diffraction pattern becomes collinear with the right He-Ne laser beam.

4.5 A second diffraction pattern is also observed on the right target. This diffraction pattern is used to control the accuracy of the alignment 2.2, where the cleaved surface of the laser array was aligned to be perpendicular to the optical axis of the external optical cavity. The second diffraction is also set up by the right He-Ne laser beam.

In the absence of the gold strip the He-Ne laser beam of 0.8 mm diameter would set up the coherent reflection, described in 2.2. However, the gold strip of 0.14 mm width intercepts the He-Ne laser beam and divides it into two sections. These two sections of the beam propagate through the lens and are reflected from the cleaved mirror face of the Ga As laser array. The two reflected beams form, in the far-field, a diffraction pattern with a single maximum and several grating lobes. A slight rotation of the mirror face of the array will result in deviating the two reflected He-Ne beam sections which then are obscured by the blackened surface of the fused silica disc. The second diffraction is easily recognized sine it does not move when the spatial filter is tilted off the normal to the optical axis. Should the second diffraction pattern not appear, then it is advisable not to proceed any further, but to slightly rotate the transformer until the diffraction pattern appears, and repeat the alignment procedure from 3.1.

4.6 The injection current is now turned up until it exceeds the threshold current for stimulated emission, (approximately 25A in the primary winding of the pulse transformer). If stimulated emission cannot be observed, slight corrections of the alignment of the lenses in the optical cavity in direction perpendicular to the p-n junction, must be made using parts A51-8019 and A51-8034. (Stimulated emission can be observed with the image converter set to infinity; it appears as a very bright spot at the center of the p-n junction.)

4.7 Finally, the output mirror is removed from part A51-8008 and the shutter is mounted. Then the output mirror is put back and aligned perpendicular to the optical axis by observing that the reflection of the left He-Ne laser on the output mirror is collinear with the laser beam.

5.1 After stimulated emission is observed, the mechanical resonator alignment in direction perpendicular to the p-n junction can be disengaged, and the electromechanical alignment control can take over.

The piezoelectric transducers for the electromechanical alignment control are mounted in the transducer housing A51-8030. Each transducer is a piezoelectric cylinder, operated in the transverse mode, of 1-inch outer diameter, 2-inch length, and 0.062-inch wall thickness. The maximum excursion is ± 7 microns for a voltage swing of ± 1000 volts.

One end of each piezoelectric cylinder is fastened to the transducer housings A51-8030 by means of part A51-8024 and the other end is connected by means of the interface couplings

A51-8029 (A51-103) to the bracket A51-8009. The transducer housings A51-8030 are held in the transducer bracket A51-8028. The transducer housings can slide in the bracket in direction perpendicular to the p-n junction.

During the alignment procedure of the laser device, the piezoelectric transducers, together with their housings A51-8030, are moved along with the brackets A51-8009.

After the alignment of the laser device is completed, first the left transducer housing A51-8030 is locked in the bracket A51-8028 and the mechanical alignment is disengaged by removing the screws in part A51-8019. Because of tensions in the laser device, the locking of the transducer moves the part A51-8008 out of alignment. This can be compensated for by the transducer coupling, 531-4000, shown in Figure 3. To do so, we mark the magnified mirror face of the Ga As laser array, set up by the left He-Ne laser on the left target, before the housing is locked. Then the housing A51-8030 is locked in the bracket A51-8028, and the part 531-4001 is rotated until the magnified mirror face had moved back into the marked position.

A similar technique can be used to compensate for tensions in the right transducer.

12. Test Procedures and Test Results

The test procedure and the test results for an array of three homostructure Ga As laser array in the spatially coherent, phase-controlled mode, are given in Section 3 and for the spatially coherent, free running mode, in Section 4. The experiments reported in Section 3 and 4 were performed using injection current pulses of 100 ns width.

Test results on homostructure lasers and laser arrays in the spatially coherent mode, at room temperature, using injection current pulses of up to 400 ns, are given in Section 7.

In this section the technique will be described of synthesizing the far-field distribution, the test results on the three-laser arrays, tested in the engineering model of the laser device, and on the four-laser arrays, tested in the laboratory model of the laser device.

12.1 Synthesized Far-Field Distribution

The technique of synthesizing the far-field distribution of the laser radiation uses the beam transformation shown schematically in Figure 3-4a. The external cylindrical lens with the focal length f_e corrects the ellipticity of the laser beam. The ellipticity is caused by the asymmetry of the p-n junctions of the laser diode array, which yields a spatially coherent beam at the output mirror of the optical cavity, in the direction perpendicular to the junctions, which is much wider than along the junctions. The focal plane of the external cylindrical lens

is at the second focal plane of the internal lens, the curvature of the cylindrical lens is in the direction of the junctions. The field distribution at the second plane of the cylindrical lens, in the direction of the junctions, is the magnified distributuion of the laser diode array where the magnification ratio is f_e/f. The cylindrical lens is an integral part of the laser device.

Using the second focal plane of the cylindrical lens as the reference plane, then the far-field distribution is the Fourier transformation of the field distribution at the second focal plane of the external cylindrical lens. It is given in general form by*

$$\mathcal{U}(r,q) = \iint G(\xi,\eta)\, e^{-j\frac{2\pi}{\lambda_0}(r\xi+q\eta)}\, d\xi\, d\eta \qquad (1)$$

where ξ and η are the coordinates of the radiating aperture and $G(\xi,\eta)$ is the field distribution over the radiating aperture (the pupil function).

---

* Born and Wolf "Principles of Optics", Pergamon Press 1964-65, Section 8.3 Eq. 38.

Further, $p = \sin\Theta_x$, $q = \sin\Theta_y$, where Θ_x and Θ_y are the angles the rays form with the normal to the aperture.

For $\xi = x_e$, $\eta = y_e$, $\sin\Theta_x = \frac{x_z}{z}$, $\sin\Theta_y = \frac{y_z}{z}$ and for the case that the pupil function represents the field distribution at the second focal plane of the external cylindrical lens, Equation 1 yields the far-field distribution of the Ga As laser array with the external cylindrical lens, in the plane perpendicular to the p-n junctions, it is

$$U_z(x_z, y_z) \propto \int_{-\infty}^{+\infty} e^{-\pi^2\left(\frac{w_{ox}}{\lambda_0 f} x_f\right)^2} \left(\int_{-2(w_{ey}+D_e)}^{-D_e} \sin\left(\frac{\pi}{2w_{ey}}(y_e - D_e)\right) + e^{j\varphi} \int_{-w_{ey}}^{w_{ey}} \cos\left(\frac{\pi}{2w_{ey}} y_e\right) \right.$$

$$\left. + e^{j\beta} \int_{D_e}^{2w_{ey}+D} \sin\left(\frac{\pi}{2w_{ey}}(y_e + D_e)\right) \right) e^{-j\frac{2\pi}{\lambda_0}\frac{x_e x_z + y_e y_z}{z}} dx_e dy_e \qquad (2)$$

where $w_{ey} = \frac{f_e}{f} w_{oy}$, $D_e = \frac{f_e}{f} D$ and z is the distance from the second plane of the cylindrical lens, in the direction of propagation. The solution of Equation 2 for the spatially coherent mode is

$$U_z(x_z, y_z) \propto e^{-\left(\frac{x_z}{w_{ox}}\frac{f}{z}\right)^2} \frac{\pi \cos\left(\frac{2\pi}{\lambda_0}\frac{w_{ey}}{z} y_z\right)}{\left(\frac{\pi}{2}\right)^2 - \left(\frac{2\pi}{\lambda_0}\frac{w_{ey}}{z} y_z\right)^2} \times$$

$$\left(1 + 2\cos\left(\frac{2\pi}{\lambda_0}\frac{y_z}{z}(w_{ey} + D)\right)\right) \qquad (3)$$

The far-field distribution could not be measured in our laboratory since Equation is valid only at a distance z, where

$$z \gg \frac{2\pi}{\lambda_0}\left(\frac{3w_{ey} + 2d_e}{2}\right)^2, \quad d_e = \frac{f_e}{f} d,$$

that is at a distance of more than 160m. Instead we have observed the synthesized far-field distribution, at the second focal plane of the external spherical lens with the focal length f_a, in Figure 3-4a. The other focal plane of this lens coincided with the second focal plane of the external cylindrical lens.

The Fourier transformation of the field distribution at the second focal plane of the external cylindrical lens, where z = 0, yields the field distribution at the second focal plane of the external spherical lens, with the focal length f_a (outlined previously). The field distribution is given by

$$\mathcal{U}_{fa}(x_a, y_a) \propto \int_{-\infty}^{+\infty} e^{-\pi^2\left(\frac{w_{ox}}{\lambda_0 f} x_f\right)^2} \left[\int_{-(2w_{ey}+D_e)}^{-D_e} \sin\left(\frac{\pi}{2w_{ey}}(y_e - D_e)\right) + e^{j\varphi_1} \int_{-w_{ey}}^{2w_{ey}} \cos\left(\frac{\pi}{2w_{ey}} y_e\right) \right.$$

$$\left. + \int_{D_e}^{2w_{ey}+D} \sin\left(\frac{\pi}{2w_{ey}}(y_e + D_e)\right) \right] e^{j\frac{2\pi}{\lambda_0}\frac{x_e x_a + y_e y_a}{f_a}} dx_e\, dy_e. \quad (4)$$

$$\mathcal{U}_{fa} \propto e^{-\left(\frac{x_a}{w_{ox}}\frac{f}{f_a}\right)^2} \frac{\pi \cos\left(\frac{2\pi}{\lambda_0}\frac{w_{ey}}{f_a} y_a\right)}{\left(\frac{\pi}{2}\right)^2 - \left(\frac{2\pi}{\lambda_0}\frac{w_{ey}}{f_a} y_a\right)^2} \times \quad (5)$$

$$\left(1 + 2\cos\left(\frac{2\pi}{\lambda_0}\frac{y_a}{f_a}(w_{ey} + D_e)\right)\right)$$

From the similarity of Equations 2 and 4 we conclude that the far-field distribution of the laser radiation can be synthesized by observing the field distribution in the second focal plane of the external spherical lens with the focal length f_a.

12.2 Three laser arrays tested in the engineering model of the laser device.

In concurrence with the design concept of the engineering model of the laser device, discrepancies in the length and in the distortions of the optical wavefronts by non-linearities in the lasers of the different arrays, were compensated with thin rings between the optical components. To optimize the optical peak pulse power using the laser array "JAP", made from the wafer 43/56, for correct spacing of the internal lenses, two rings of 48 and 15.4 mil thickness are placed between the building block A51-8007 and the right bracket A51-8009, and one ring of 53.5 mil is placed between the building block A51-8008 and the left bracket A51-8009. For correct spacing of the spatial filter, a ring of 77 mil thickness is placed in building block A51-8007 to control the location of part 531-4008, and two nylon rings of 18 and 16 mil thickness are placed in building block A51-8008 to control the location of the output mirror.

The optical peak pulse power of the three laser array in the spatially coherent, free running mode, is close to 5 watts. The peak injection current is approximately 180A (Figure 12-1). The measured peak power is, in fact, three times the typical peak power of a single laser of the dimensions of the lasers in the array.

It seems of interest to compare the two measurements which were made using the same three laser array. That is the measurement made when the laser array was operated in the laboratory model of the laser device (Section 4 Figure 6) and when operated in the engineering model, Fig. 12-1.

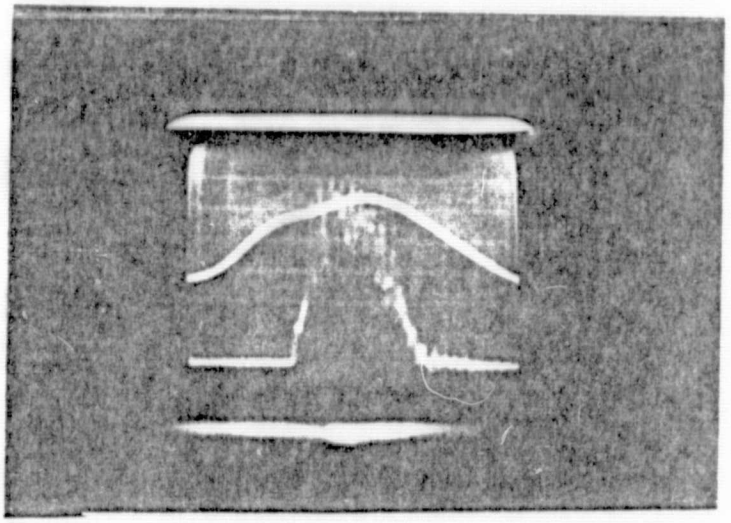

Upper vertical trace: 60 A/div

Lower vertical trace: 1 W/div

Horizontal trace: 20 ns/div

Fig. 12-1 Injection current and optical waveform of three laser array JAP in spatially coherent, free running mode. Spatial filter:140 microns, aperture at output mirror: 1000 microns. Laser array operated in laser device

There is great similarily between the two waveforms, even the knee, which indicates the on-set of stimulated emission of the outer lasers, seems to occur at the same injection current level.

Also, the symthesized far-field distribution of the laser array, operated in the engineering model, was similar to that given in Section 4, Figure 7.

However, it should be mentioned that the results prese-ted in this section, Figure 12-1, could only be obtained when a shutter of 1000 microns width was placed in the building block A51-8008, in front of the output mirror. A similar shutter was not used to obtain the result in Section 4, Figure 6. Without shutter, the optical peak pulse power of the three laser array in the engineering model was only approximately 3.3 watts, as shown in Figure 12-2.

The shutter had been added to eliminate the two modulation sidebands which appear at a distance of approximately 800 microns from the optical axis, in the plane of the array, on the output mirror. These modulation sidebands result from a spatial modulation in the plane of the p-n junction of the lasers. The origin of the spatial modulation is being studied.

To optimize the optical peak pulse power using the laser array "F", made from wafer 43/56, for correct spacing of the lenses, two rings of 48 and 15.7 mil thickness are placed between the building block A51-8007 and the right bracket A51-8009, and one ring of 53.5 mil thickness between building block A51-8008 and the left bracket A51-8009. For correct spacing of the

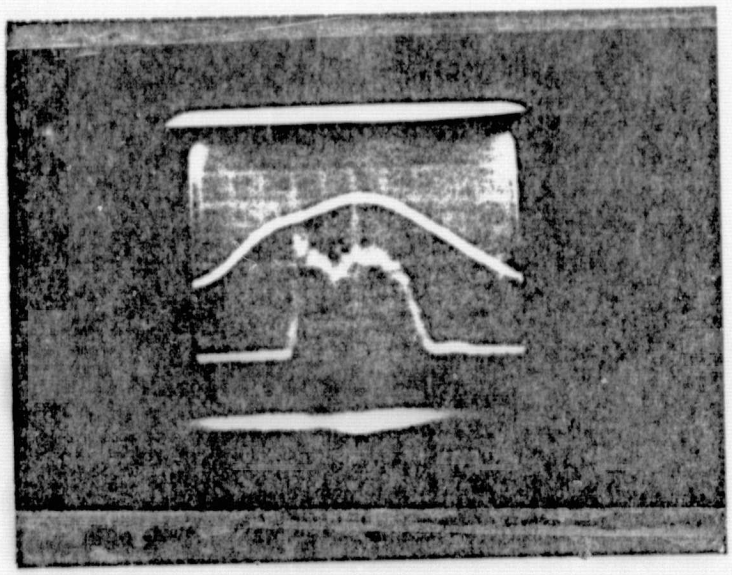

Upper vertical trace: 60 A/div

Lower vertical trace; 1 W/div

Horizontal trace: 20 ns/div

Fig. 12-2 Injection current and optical waveform of three laser array JAP in spatially coherent, free running mode. Spatial filter: 140 microns, laser array operated in laser device

spatial filter a ring of 77 mil thickness is placed in building block A51-8007 to control the location of part 531-4008, and three nylon rings of 18, 18 and 16 mil thickness are placed in building block A51-8008 to control the location of the output mirror.

The optical peak pulse power of the three laser array in the spatially coherent, free running mode, is close to 5 watts, when the shutter of 1000 microns width was placed in front of the output mirror. The peak injection current is approximately 180A (Fig. 12-3).The measured peak power is, in fact, three times the typical peak power of a single laser of the dimensions of the lasers in the array.

In addition to evaluating the synthesized far-field of the laser array, which is similar to that in Section 4, Figure 7, we have also investigated the intensity distribution of the spatially coherent beam at a distance of 18 m from the second focal plane of the external cylindical lens, with 21 cm focal length. (This was all the space we had.) The image of the laser beam on a photographic plate is shown in Fig. 12-4. The density distribution of the image was recorded, using a micro-densitometer; it is shown in Figure 12-5.

At the second focal plane of the external cylindrical lens, the field distribution in the plane of the array, is that of the array itself but magnified by the ratio of the focal lengths of the external lens (fe) and the internal lens (f). For fe = 21 cm and f = 1 cm, the magnified width of each laser in the array is $2 W_{ey} = 0.4$ cm and the Gaussian mode width, where the field is e^{-1}, that if the field maximum is 0.21cm. The spacing between lasers becomes $S_e = 0.484$ cm.

C-2

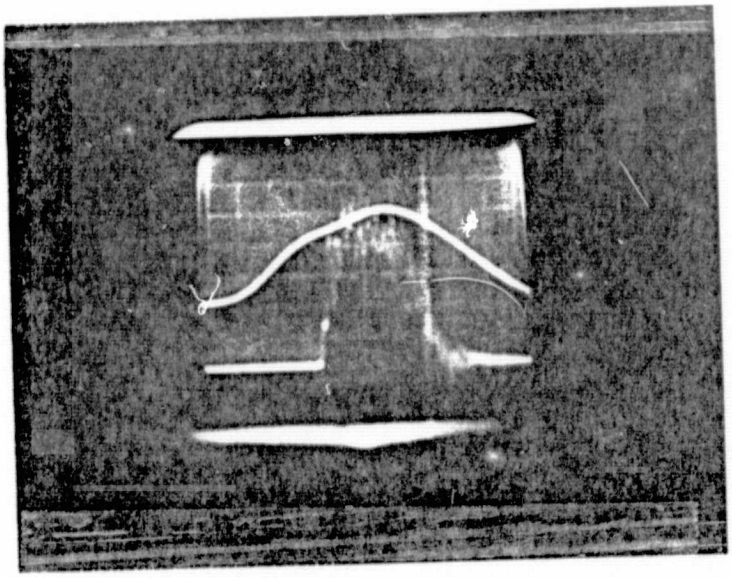

Upper vertical trace: 60 A/div

Lower vertical trace: 1 W/div

Horizontal trace: 20 ns/div

Fig. 12-3 Injection current and optical waveform of three laser array F in spatially coherent, free running mode. Spatial filter: 130 microns, aperture at putput mirror: 1000 microns. Laser array operated in laser device.

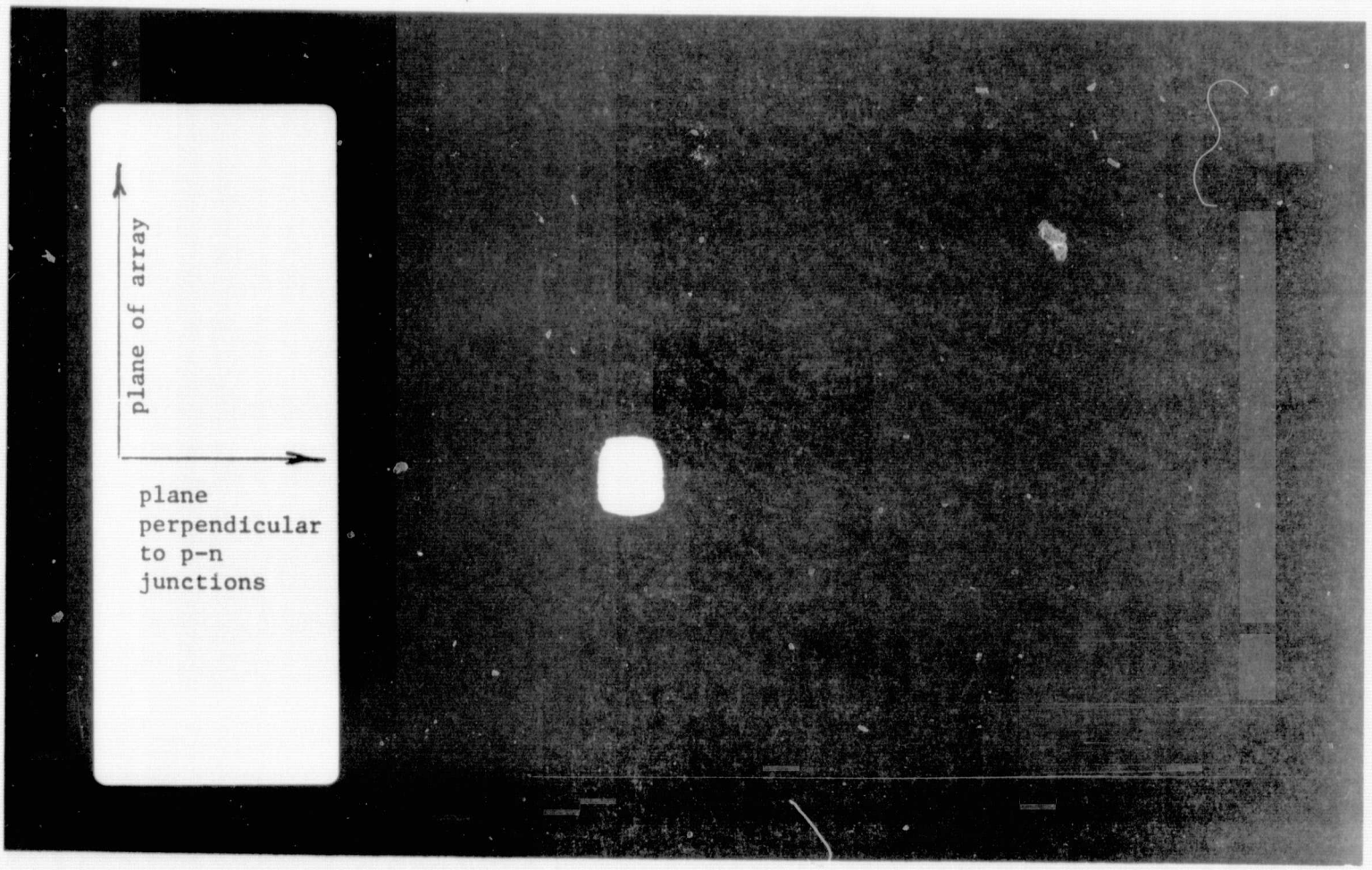

Fig. 12-4 Intensity distribution, at a distance of 18 m from the second focal plane of the external cylindrical lens, of three laser array F, in the spatially coherent, free running mode.

Fig. 12- 5 Density distribution of image of laser beam, at a distance of 18 m from second focal plane of external cylindrical lens, of three laser array F, in spatially coherent, free running mode. Spatial filter: 140 microns, aperture at output mirror: 1000 microns

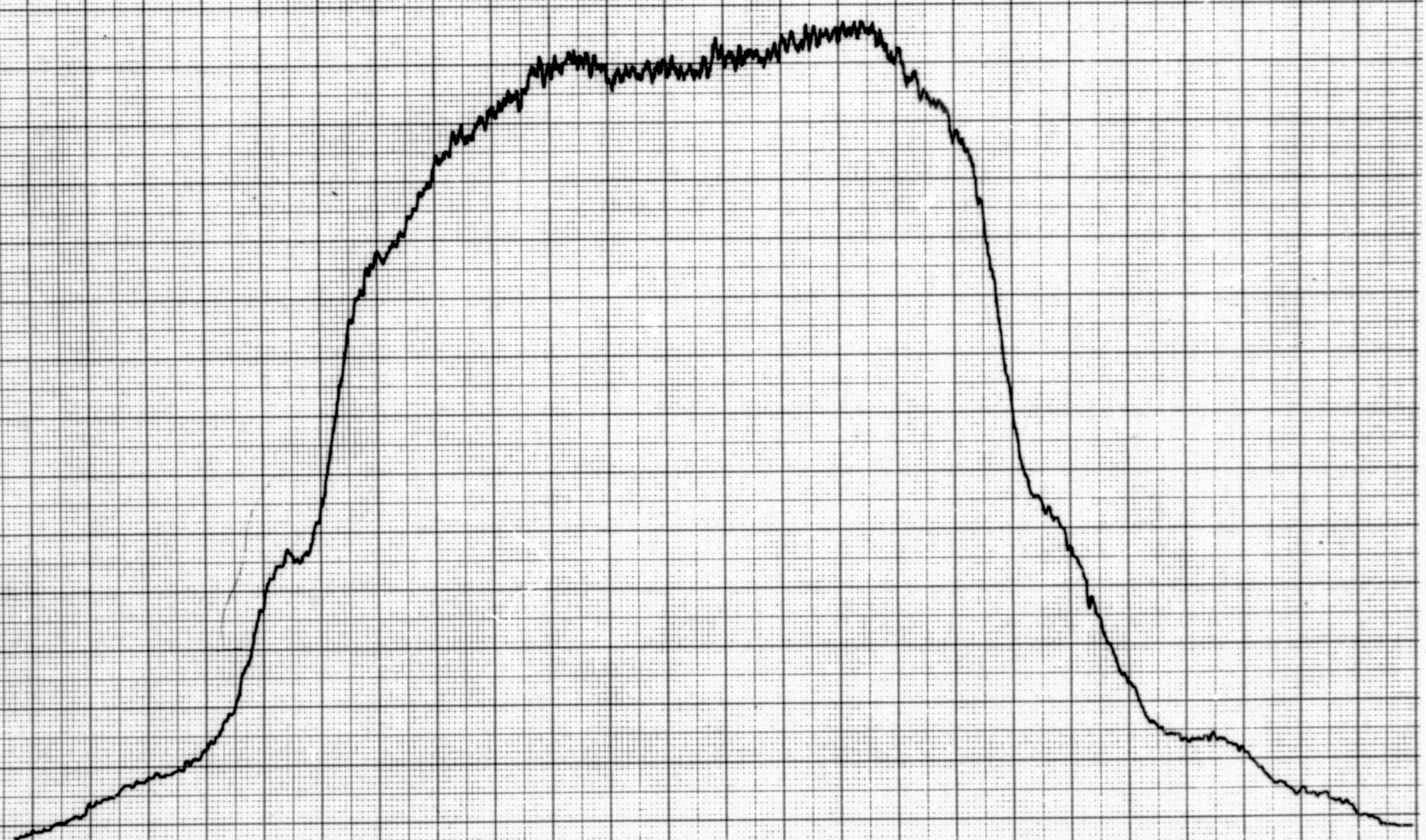

The spatially coherent waves from the three lasers in the array propagate from the second focal plane of the external cylindrical lens, with their propagation paths parallel to the optical axis. The waves expand as they propagate in space but their maxima remain stationary, spaced at a distance 0.484 cm apart. At a distance of 18 m the Gaussian mode width of each laser beam becomes 1 cm, so that the wave expansion already exceeds the spacing between the radiation maxima. The fields of the three lasers are partly superimposed at this distance. However, no interference between the optical fields can be observed.

To optimize the optical peak pulse power using the laser array 43/56, made from wafer 43/56, for correct spacing of the lenses, two rings of 48 and 16 mil thickness are placed between the building block A51-8007 and the right bracket A51-8009, and one ring of 53.5 mil thickness between building block A51-8008 and the left bracket A51-8009. For correct spacing of the spatial filter a ring of 85 mil thickness is placed in building block A51-8007 to control the location of part 531-4008, and one nylon ring of 18 mil together with 4 nylon rings of 16 mil thickness are placed in building block A51-8008 to control the location of the output mirror.

The peak pulse power of the three laser array in the spatially coherent, free running mode, was only measured without the shutter at the output mirror. It is approximately 3.5 watts Fig. 12-6. We can extrapolate from the characteristics of the laser arrays JAP and F, which were made from the same wafer, that the optical power of the laser device with the array 43/56 will also increase to 5 watts, should a shutter be placed in front of the output mirror.

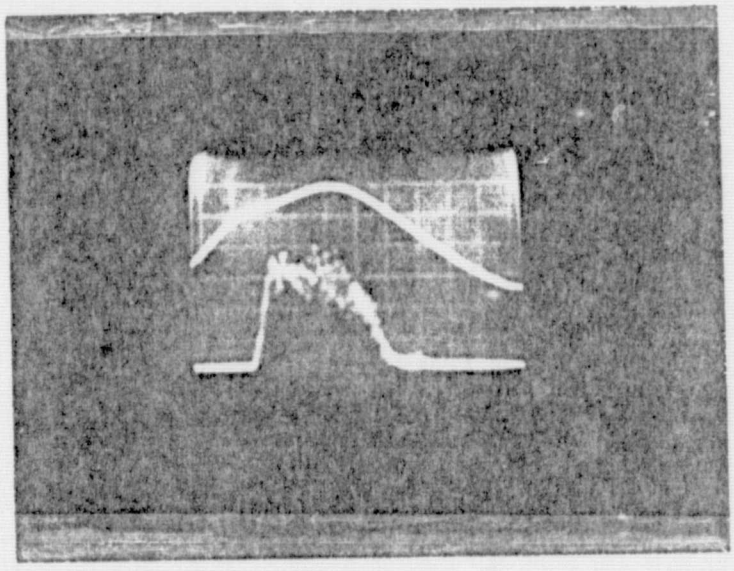

Upper vertical trace: 60 A/div

Lower vertical trace: 1 W/div

Horizontal trace: 20 ns/div

Fig. 12-6 Injection current and optical waveform of three laser array 43/56 in spatially coherent, free running mode , spatial filter: 140 microns, laser array operated in laser device

The synthesized far-field distribution is similar to that in Section 4, Figure 7 .

To optimize the optical peak pulse power using the laser array 24/37, made from wafer 24/37, for correct spacing of the lenses, three rings of 48, 15.1 and 1 mil thickness are placed between the building block A51-8007 and the right bracket A51-8009, and one ring of 53.5 mil thickness between building block A51-8008 and the left bracket A51-8009. For correct spacing of the spatial filter a ring of 77 mil thickness is placed in building block A51-8007 to control the location of part 531-4008, and two nylon rings of 18 mil, together with two nylon rings of 16 mil thickness are placed in building block A51-8008 to control the location of the output mirror.

The peak pulse power of the three laser array in the spatially coherent, free running mode, was only measured without shutter at the output mirror. It is close to 4 watts. Fig. 12-7.

The synthesized far-field distribution similar to that in Section 4, Figure 7.

To optimize the optical peak pulse power using the laser array "Glint" made from wafer 29/54, for correct spacing of the lenses, three rings of 48, 15.4 and 2 mil thickness are placed between the building block A51-8007 and the right bracket A51-8009, and one ring of 53.5 mil thickness between building block A51-8008 and the left bracket A51-8009. For correct spacing of the spatial filter a ring of 77 mil thickness is placed in building block A51-8007 to control the location of part 531-4008, and two nylon rings of 18, and 16 mil thickness are placed in building block A51-8008 to control the location of the output mirror.

The peak pulse power of the three laser array in the spatially coherent, free running mode, was measured with and without a

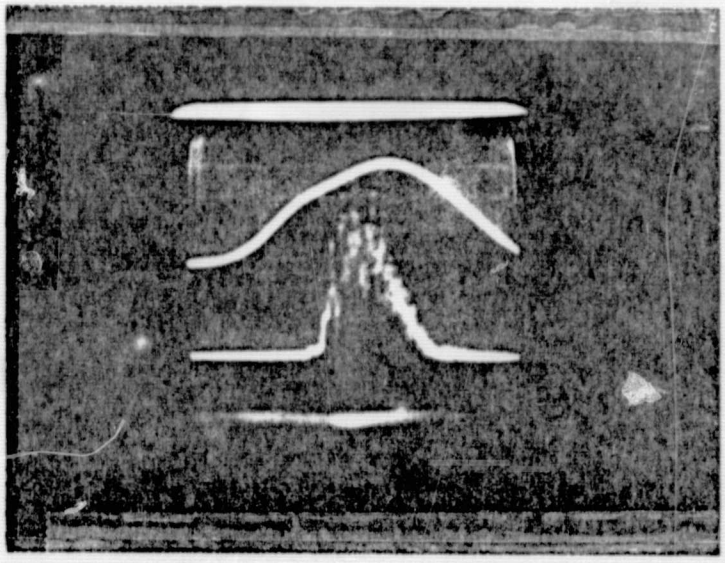

Upper vertical trace: 60 A/div
Lower verticaltrace: 1 W/div
Horizontal trace: 20 ns/div

Fig. 12-7 Injection current and optical waveform of three laser array 24/37 in spatially coherent, free running mode, spatial filter 140 micro Laser array was operated in laser device

shutter of 700 microns at the output mirror. It is approximately 3.5 watts as shown in Fig. 12-8, whether or not the shutter was used. Through the shutter did not increase the optical peak pulse, it slightly increased the optical pulse length.

The wafer 29/54 was diffused in a different time period than the wafer 43/56, so their characteristics can possibly be quite different. Also, the wafer 29/54 is only 2.3 mil high and the alignment of the laser device is more difficult when the "Glint" array is used, especially the alignment to the center of the optical resonator using the spontaneous emission of the diodes.

The synthesized far-field distribution is similar to that in Section 4, Figure 7.

12.3 Four Laser Array

The technique of spatially coherent beam formation from an array of Ga As lasers in the free running mode, has also been extended to an array of four diffused homostructureGa As lasers of 8 mil width. The measured peak pulse power, at room temperature, was 5 watts. Since the power from the four laser array should be in excess of 6 watts, it seemed important to investigate the cause of the power limitation.

It has been observed that the two outer lasers in the array exceeded threshold at a lower injection current than the two inner lasers. Should this effect be introduced by spherical aberrations of the internal lenses in the cavity, then an increase in distance between the internal lenses and the plane mirrors of the optical cavity, would reduce the threshold current for the two inner lasers. This assumption was verified and a mirror spacing was found experimentally, where the threshold current for

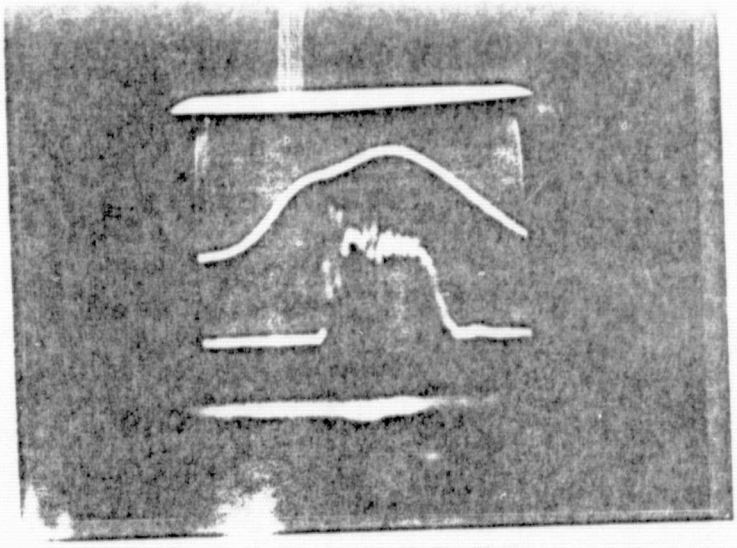

Spatial filter: 140 microns, aperture at output mirror: 700 micr

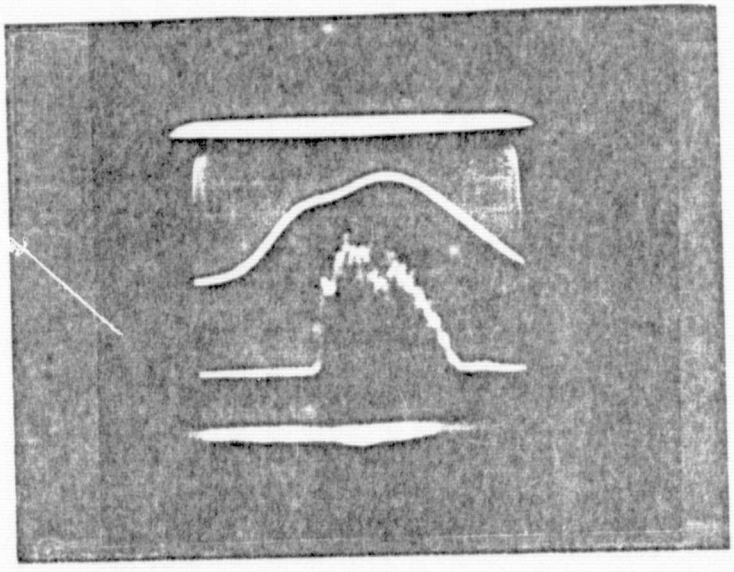

Spatial filter: 140 microns

Upper vertical trace: 60 A/div
Lower vertical trace: 1 W/div
Horizontal trace: 20 ns/div

Fig. 12-8 Injection current and optical waveform of three laser array Glint, in spatially coherent, free running mode. Laser array is operated in laser device.

the four lasers in the array, was closely the same. However, this spacing is not the optimum spacing for any of the lasers in the array.

We conclude that, because of the spherical aberration in the uncorrected lenses of the laser device, a four laser array will not operate efficiently in the laser device. For arrays with more than three lasers, doublets which are corrected for spherical aberrations, should be used in the laser device.

APPENDIX

Evaluation of Thermo-electric Cooler for Ga As Laser Array

The feasibility had been investigated of incorporating a thermo-electric cooler in the laser device which had been developed under NASA contract NAS 8-11974. The objective of this investigation was to determine whether a thermo-electric cooler can be added without major changes in the design of the laser device. The thermo-electric cooler seemed to be required to extend the duration of the optical pulses to 400 ns, when an array of homostructure lasers is used.

It had been outlined in the proposal of August 14, 1973, that, at room temperature, optical pulses of 400 ns duration in the spatially coherent mode can only be attained when hetero-structure lasers are being used. However, no heterostructure laser material could be obtained during the duration of this contract, which could be used efficiently for a spatially coherent laser array, as outlined in Section .

Tests had been performed on a homostructure Ga As laser of 200 microns width in the spatially coherent mode. Standard heat sinks were used and the injection current pulses were not especially shaped. Optical pulses of close to 300 ns duration could be obtained with fairly uniform intensity distribution of 1.5 watts. The uniform intensity distribution required transverse mode control at both plane mirrors of the external optical cavity.

The homostructure Ga As lasers used for both tests were made from a wafer with especially low threshold current density, which had been diffused and processed at IBM-FSD Gaithersburg.

This material, however, is used up and the material available to us has higher threshold current densities. For this material cooling will be required to obtain optical pulses of several hundred nano-seconds.

From the analysis on temperature behavior in p-n junction laser we have derived that an increase in optical pulse length to 400 ns cannot be accomplished by improving the heat sink design or the heat sink material but only by keeping the p-n junctions at temperatures below room temperature. Heat is produced in the p-n junction at a rate which is proportional to the product of gap voltage times injection current. The temperature of the p-n junction begins to rise as the injection current is turned on, proportional to the square root of time. The thermal energy also starts penetrating into the adjacent p- and n- regions of the laser, but very little heat penetrates further than the distance x, which also is proportional to the square root of time. The penetration depth x in the Ga Sa laser approaches 7 microns after 400 ns, but the distrance between the p-n junction and the heat sink in the homostructure lasers which had been diffused in our laboratories, is 18 to 25 microns. Because of the small penetration depth, the heat sink of the laser cannot influence the transfer of heat from the p-n junction to the surrounding material.

External cooling of the Ga As laser reduces its temperature and also its threshold current. Thus, the temperature rise during the injection current pulses starts from a lower value and also the thermal energy generated in the p-n junction is smaller.

The construction of the laser device developed under NASA contract NAS 8-11974 is such that the Ga As lasers are held in

the pulse transformer (part 8015-37). The heat generated in the p-n junction of the Ga As lasers is transferred through the p- region to the large cooper heat sink which is part of the transformer cover (part L99204). The cold junction of a thermo-electric cooler can be bonded directly to part L99204. The hot junction can be connected by means of a soft spring contact to the large metal part A51-8028 which holds the piezo-electric transducers. The alignment mechanism of the laser device will not be impaired by the thermo-electric cooler since it can move together with the transformer.

Cooling of the Ga As laser array will require to enclose the laser device with a cover in order to avoid condensation on the mirror faces of the lasers. The cover can be bonded to the base plate (part 8027) and the enclosed volume can be filled with dry nitrogen. The external cylindrical lens would become part of the cover to transmit the laser light. The piezo-electric crystals would be inside the cover, and the high voltage connectors would be provided with vacuum seals.

The heat pumping load was evaluated and an attempt is being made to minimize it by thermo-isolating the transformer in the laser device. To accomplish this, the block, part 8014, which seats the transformer in the housing and the clamp, part 8039, which tightens the transformer to the block, should be made of plastic material with low thermal conductivity. Also the transformer should be covered with a sleeve of the same plastic material. The addition of the plastic sleeve requires a reduction of the outer dimentsions of the transformer, especially of the outer diameter of the housing, part A51-8015, and an increase of the round opening in the block, part A51-8014.

The heat flow in the thermo-isolated transformer will be primarily by conduction on two separate paths. Heat will flow in axial direction from the housing with the temperature T_1 through the block, part A51-8014, and through the transformer housing, part A51-8015, to the transformer cover, part L99204 which is at the temperature T_2. Heat also flows in radial direction from the surrounding air of the temperature T_1 through the thermal isolation to the transformer housing, part A51-8015, of the temperature $T \approx T_2$.

For the axial heat flow the temperature at the interface between transformer housing A51-8015 and the plastic part A51-8014, using epoxy glass, is

$$T_m = \frac{\frac{k_1}{L_1} T_1 + \frac{k_2}{L_2} T_2}{\frac{k_1}{L_1} + \frac{k_2}{L_2}} \qquad (1)$$

where k_1 and k_2 are the thermal conductivities of epoxy glass and copper; L_1 and L_2 are the lengths of part A51-8014 and part A51-8015; $k_1 = 2.6 \times 10^{-3}$ W cm^{-1} (^{o}K)$^{-1}$ and $k_2 = 5$ W cm^{-1} (^{o}K)$^{-1}$. For $L_1 = 0.9$ cm and $L_2 = 2.5$ cm, $T_1 = 300^{o}$ K and $T_2 = 270^{o}$K, $T_m \approx T_2$. The heat flow from the invar housing to the transformer cover, part 8021, is

$$q = \frac{A(T_1 - T_2)}{\frac{L_1}{k_1} + \frac{L_2}{k_2}}$$

where A is the cross section of the transformer housing, part 8015, $A \approx 0.755$ cm^2. Then the heat flow in axial direction is

$$q = 66 \text{ mW}$$

The thermo-isolation which reduces the radial heat flow is in the form of a sleeve of epoxy glass. The thermo-electricl sleeve is not completely attached to the transformer housing, but

is under-cut so that an air layer of lower thermal conductivity is formed between the copper transformer housing and the epoxy glass sleeve. The spacers which hold the sleeve concentric with the transformer housing, must be very thin. Then the radial heat flow can be approximated by

$$q = \frac{2\pi L_2 (T_1 - T_2)}{\frac{\ln \frac{r_m}{r_2}}{k_{2_2}} + \frac{\ln \frac{r_1}{r_m}}{k_{2_1}}} \qquad (2)$$

where L_2 is the length of the transformer housing, (L_2 = 2.5 cm), r_1 and r_m are the outer and inner radii of the epoxy glass sleeve, (r_1 = 0.9 cm, r_m = 0.8 cm) r_2 is the outer radius of the transformer housing, (r_2 = 0.7 cm), the thermo-conductivities of air is k_2 = 0.000275 W cm^{-1} $(^oK)^{-1}$. For T_1 = 300°K and T_2 = 270°K, the radial heat flow from Equation 2 is 1 watt.

The heat pumping capacity of the thermo-electric cooler must also compensate for the average power dissipated by the Ga As lasers. For a three-homostructure laser array, the average dissipated power is approximately 0.12 watt.

To complete the thermo-analysis, the thermal contraction of the transformer which holds the p-n junction lasers, part A51-8015, has to be evaluated. Because of the thermo-isolation required to minimize the heat pumping capacity of the thermo-electric cooler, the transformer temperature will be close to 270°K over the entire length of the transformer. The change in transformer length from its room temperature value L_T is

$$L_{T-\Delta T} = (1 - \beta \Delta T) L_T .$$

A reduction in temperature by $30^{o}K$ will reduce the transformer length by 12 microns, for L_T = 2.5 cm and $\beta = 0.159 \times 10^{-4}\ {}^{o}K^{-1}$.

To avoid major changes in the design, the laser device should be aligned at room temperature and the thermo-electric cooler should be activated after the device is covered and filled with nitrogen. To compensate for the thermal contraction of the transformer, the lens-mirror combination parts A51-8007 and A51-8008 must then be moved towards the housing by approximately 12 microns by means of the screws, in parts A51-8019 and A51-8034. After the laser device with the activated thermo-electric cooler has come to the thermo-equilibrium, the piezo-electric transducer must be used for precision alignment of the laser device.

A typical thermo-electric cooler to be used with the laser device is CAMBION Model 801-3960-01. The cooler is able to maintain 2.1 watts heat pump rate across a 32^{o} C temperature differential for a hot junction temperature of 30^{o}C. The cooler weight is 10 grams, its size is 0.65 x 0.85 x 0.21 in., it is consuming approximate 4 Amperes at 1 Volt d.c.

This thermo-electric cooler has the general characteristics required for use in the laser device, but its dimensions are not too well matched to the dimensions of the transformer cover, part A51-8021. An attempt will be made to find a thermo-cooler with better match to the transformer cover.